Infrared temperature sensing of snow covered terrain
by Bernard Allen Shafer

A thesis submitted to the Graduate Faculty in partial fulfillment of the requirements for the degree of MASTER OF SCIENCE in Earth Science (Meteorology)
Montana State University

Abstract:
The feasibility of remotely monitoring snow surface temperatures with a Barnes IT-3 infrared thermometer was investigated. Much of the work concentrated on determining the vertical emissivity of dry snow in the atmospheric infrared "window" region between 8 and 14 microns.

The emissivity of various snow surface types was measured using an apparatus called an "emissivity box." An average emissivity for freshly fallen snow was found to be 0.975® For snow surfaces crusted by the effects of wind or melt phenomenon the average emissivity was 0.985. The mean emissivity for all snow surface types examined was 0.978. These high emissivity values substantiate the hypothesis that snow possesses approximately blackbody characteristics in the 8 to 14 micron spectral interval.

An analysis of errors in radiometrically obtained snow surface temperatures revealed that the IT-3 is capable of accurately measuring the true surface temperature to within two degrees Celsius for the temperature range experienced. Inversions in snow covered mountain valleys were successfully mapped during airborne case studies. Tops of inversions were located by measuring the snow surface temperature variation with elevation and noting the intersection of the inversion top with the mountain slope.

Remote radiometric temperature sensing of snow surfaces appears to offer a potentially useful tool for monitoring surface temperature gradients in arctic environments. Its application to meteorological investigations of surface temperature variation in otherwise inaccessible mountainous regions in winter may also prove valuable.

PERMISSION TO COPY

In presenting this thesis in partial fulfillment of the requirements for an advanced degree at Montana State University, I agree that the Library shall make it freely available for inspection. I further agree that permission for extensive copying of this thesis for scholarly purposes may be granted by my major professor, or, in his absence, by the Director of Libraries. It is understood that any copying or publication of this thesis for financial gain shall not be allowed without my written permission.

Signature Bernard Allen Shafer

Date 5/19/71

INFRARED TEMPERATURE SENSING OF SNOW COVERED TERRAIN

by

Bernard Allen Shafer

A thesis submitted to the Graduate Faculty in partial fulfillment of the requirements for the degree

of

MASTER OF SCIENCE

in

Earth Science (Meteorology)

Approved:

Milton J. Edie

Head, Major Department

Arlin B. Super

Chairman, Examining Committee

Graduate Dean

MONTANA STATE UNIVERSITY
Bozeman, Montana

June, 1971

ACKNOWLEDGMENT

My sincere thanks go to Dr. A.B. Super for suggesting this thesis problem and for providing support from ERF Project 620. He is also accorded thanks for his encouragement and guidance during the course of the investigation and for his constructive criticism of the thesis manuscript. Gratitude is extended to Dr. W.B. Bendel and Dr. W. Hunt for reading the thesis manuscript and making helpful suggestions. Appreciation is also extended to other members of my graduate committee who made pertinent and helpful comments in the preparation of the thesis.

My thanks to Dr. K. Buettner and Dr. K. Katsaros of the Department of Atmospheric Sciences, University of Washington, for the loan of the emissivity box and for valuable comments on the technique of making emissivity measurements.

To my wife, Connie, a special thanks for all the many hours spent typing thesis drafts and the final manuscript. Her patience, understanding, and good humor helped immeasurably.

TABLE OF CONTENTS

	Page
Vita	ii
Acknowledgment	iii
Table of Contents	iv
List of Tables	vi
List of Illustrations	vii
Definition of Symbols	ix
Abstract	xii
Chapter 1: Introduction	1
1.1 General Remarks	1
1.2 Definition of the Problem	5
Chapter 2: Survey of Recent Infrared Temperature Sensing Investigations and Elementary Radiation Theory	12
2.1 General Remarks	12
2.2 Elementary Radiation Theory and Definition of Terms	16
2.3 Spectral Emissivity and Total Emissivity of Snow	22
Chapter 3: Description of Radiometer	27
3.1 General Description of Radiometer and Recorder	27
3.2 Spectral Response of the IT-3	30
3.3 Calibration of the Radiometer	36
Chapter 4: Emissivity of Snow Surfaces	42
4.1 General Remarks	42

Page

4.2 Design of Measurement Technique 44

4.3 Discussion of Errors 52

4.4 Replication of Snow Crystals 58

4.5 Results of Emissivity Investigations 60

Chapter 5: The Effect of Reflected Radiation and Atmospheric Absorption 65

5.1 General Remarks 65

5.2 The Effect of a Clear Sky 66

5.3 The Effect of a Cloud Covered Sky 70

5.4 The Effect of Nearby Objects and Atmospheric Attenuation 73

Chapter 6: Airborne Temperature Measurements Over Snowfields . . . 75

6.1 General Remarks 75

6.2 Results of Aerial Measurements 76

Chapter 7: Summary and Recommendations for Further Study 87

Literature Cited 91

LIST OF TABLES

		Page
Table 2.1	Normal emissivities of natural surfaces in the atmospheric infrared window between 8 and 14 microns	14
Table 2.2	Definition of radiation terminology	17
Table 4.1	Induced error in emissivity caused by radiative heating of the snow surface with the black lid in place	54
Table 4.2	The effect of temperature variation on the calculated emissivity of a snow surface at -3C	56
Table 4.3	Comparison of spectral emissivities for similar surfaces in the 8 to 14 micron region	57
Table 4.4	Average emissivities for various snow surfaces and crystal types	61
Table 6.1	Comparison of radiant snow surface temperature, "surface" temperature obtained with a precision thermometer, shelter temperature, and air temperature at flight level over a snowfield at night	84

LIST OF ILLUSTRATIONS

Page

Figure 1.1 The electromagnetic spectrum and an expansion of the infrared region showing wavelength of maximum or peak emission for indicated temperatures 6

Figure 1.2 Spectral locations of atmospheric infrared "windows" . . 7

Figure 1.3 Temperature difference between the true surface temperature and the temperature indicated by a radiometer as a function of emissivity and surface temperature 9

Figure 2.1 Blackbody radiation curves for the temperature range commonly experienced by natural surfaces 19

Figure 2.2 Vertical reflectance curves for water and a smooth ice surface due to Weingeroff (1931) as reported by Buettner and Kern (1965) 24

Figure 3.1 Transmission curve of PRT-5 which is similar to that of the IT-3 (after Dana, 1969) 31

Figure 3.2 Spectral radiant emittance of a blackbody at 253K sensed by IT-3 31

Figure 3.3 Effective blackbody radiance B(T) versus temperature for the Barnes IT-3 33

Figure 3.4 Transmission characteristics of the atmosphere for typical concentrations of water vapor, carbon dioxide, and ozone (after Gates, 1962) 35

Figure 3.5 Diagram of blackbody calibration chamber. Photograph of the blackbody cavity and its housing 37

Figure 3.6 Calibration setup for the low temperature range 39

Figure 3.7 Calibration setup for the high temperature range 39

Page

Figure 3.8 Calibration curve for the Barnes IT-3 infrared thermometer showing temperature versus millivolt output 40

Figure 4.1 Diagram of the emissivity box and radiometer arrangement to determine the emissivity of the surface forming the floor of the cylinder 46

Figure 4.2 Photograph of the snow boards and the area where the snow samples were collected 53

Figure 4.3 Photograph of the arrangement of the emissivity box, radiometer, and snow sample in preparation for a set of measurements 53

Figure 5.1 Spectral radiance of a clear sky for elevation angles of 0°, 1.8°, 3.6°, 7.2°, 14.5°, 30°, and 90° (after Bell _et al._, 1960) 68

Figure 5.2 Plot of radiant sky temperature versus elevation on February 2, 1971, at Bozeman, Montana, elevation 5,000 feet above sea level 71

Figure 6.1 Plot of the radiant snow surface temperature obtained with an airborne IT-3 radiometer for a cross sectional profile of the Gallatin Valley, Montana 77

Figure 6.2 Reconstruction of the vertical air temperature profile existing above the Gallatin Valley during the aerial observation of January 12, 1971 79

Figure 6.3 Plot of the radiant snow surface temperature obtained with an airborne IT-3 radiometer in the Centennial Valley of southwestern Montana on March 6, 1971 81

DEFINITION OF SYMBOLS

Symbol	
a_λ	Absorptivity at wavelength λ.
$B^*(\lambda,T)$	Planck function for the radiant emittance of a blackbody.
$B(\lambda,T)$	Planck function for the radiance of a blackbody.
$B(T)$	Effective blackbody radiance sensed by a radiometer.
B_f	Effective blackbody radiance from the material forming the floor of the emissivity box.
B_r	Effective blackbody radiance from the roof of the emissivity box.
B_r^b	Effective blackbody radiance from the roof of the emissivity box with the black lid exposed.
B_r^m	Effective blackbody radiance from the roof of the emissivity box with the mirror lid exposed.
c	Velocity of light in a vacuum, 2.997925×10^8 (m/sec).
C_1	First constant in Planck function for radiant emittance of a blackbody, 3.7105×10^4 (watts-micron^4/cm^2).
C_2	Second constant in Planck function for radiant emittance of a blackbody, 1.43879 (microns-°K).
$E(\lambda,T_s)$	Spectral radiant emittance from a graybody.
$G(\lambda,T_a)$	Spectral radiant emittance from the sky.
h	Planck's constant, 6.6256×10^{-34} (joule-sec).
IRT	Infrared thermometer.
IT-3	Barnes Engineering Company's Infrared Thermometer.
k	Boltzmann constant, 1.38047×10^{-16} (erg/°K).

Symbol	
N	Total radiance from a graybody.
N_{bb}	Total radiance from a blackbody.
N_f	The radiance from the floor of the emissivity box upward.
N_r	The radiance from the roof of the emissivity box downward.
N_s	The radiance from a snow surface sensed by the IT-3, including the reflected component from the sky.
N_f^b	The radiance from the floor of the emissivity box when the black lid is exposed.
N_f^m	The radiance from the floor of the emissivity box when the mirror lid is exposed.
N_r^b	The radiance from the roof of the emissivity box with the black lid exposed.
PRT-5	Barnes Engineering Company's Portable Radiation Thermometer.
$q(\lambda)$	Filter response of radiometer which defines the spectral transmission characteristics of the radiometer.
r_λ	Reflectivity at wavelength λ.
r_s	Average reflectivity for a given spectral interval.
t_λ	Transmissivity at wavelength λ.
T	Temperature in degrees Kelvin.
T_s	Temperature of a given surface.
T_f	Temperature of material forming the floor of the emissivity box.
T_r	Temperature of the roof of the emissivity box.
T_a	Average temperature of the sky.
W	Total radiant emittance from a graybody.

Symbol	
W_{bb}	Total radiant emittance from a blackbody.
ϵ_λ	Emissivity at wavelength λ.
ϵ_f	Average spectral emissivity of the material forming the floor of the emissivity box.
ϵ_s	Average emissivity for a given spectral interval.
ϵ_t	Total average emissivity.
ϵ_r^m	Average spectral emissivity of the roof of the emissivity box with the mirror lid exposed.
ϵ_r^b	Average spectral emissivity of the roof of the emissivity box with the black lid exposed.
λ	Wavelength (microns).
λ_{max}	Wavelength of maximum emission from a blackbody at a given temperature.
π	3.1416
σ	Stefan-Boltzmann constant, 5.6698×10^{-12} (watts/cm^2-$^\circ$K^4).

ABSTRACT

The feasibility of remotely monitoring snow surface temperatures with a Barnes IT-3 infrared thermometer was investigated. Much of the work concentrated on determining the vertical emissivity of dry snow in the atmospheric infrared "window" region between 8 and 14 microns.

The emissivity of various snow surface types was measured using an apparatus called an "emissivity box." An average emissivity for freshly fallen snow was found to be 0.975. For snow surfaces crusted by the effects of wind or melt phenomenon the average emissivity was 0.985. The mean emissivity for all snow surface types examined was 0.978. These high emissivity values substantiate the hypothesis that snow possesses approximately blackbody characteristics in the 8 to 14 micron spectral interval.

An analysis of errors in radiometrically obtained snow surface temperatures revealed that the IT-3 is capable of accurately measuring the true surface temperature to within two degrees Celsius for the temperature range experienced. Inversions in snow covered mountain valleys were successfully mapped during airborne case studies. Tops of inversions were located by measuring the snow surface temperature variation with elevation and noting the intersection of the inversion top with the mountain slope.

Remote radiometric temperature sensing of snow surfaces appears to offer a potentially useful tool for monitoring surface temperature gradients in arctic environments. Its application to meteorological investigations of surface temperature variation in otherwise inaccessible mountainous regions in winter may also prove valuable.

Chapter 1

INTRODUCTION

1.1 General Remarks

Temperature in the zone from the surface of the earth to approximately two meters above the surface is important for many reasons. In this layer in which animal and plant life abound, temperature is one of the primary factors of their environment. Man is intimately affected by the temperature in this layer where he conducts nearly all of his daily activity. The type of clothing he wears, the crop he grows for food, and the transportation he utilizes to travel to his destination, all depend significantly on the temperature in this region.

To say that this zone is characterized by a unique temperature is, however, misleading and an oversimplification. In reality, the temperature of the surface may be substantially different than that at a height of one or two meters. The vertical temperature gradient which exists in the lowest two meters at any given location at a particular time is a function of many variables. The most important of these variables is wind speed (Geiger, 1966). Increased wind speeds tend to produce a well mixed layer of air in which temperature is relatively homogeneous except for perhaps a small layer of a few millimeters in depth immediately above the surface. The existence of this layer near the surface is attributed to frictional forces resulting from the motion of air over the surface. The distribution of temperature in the zone between the surface and a height of two meters represents a complex problem and is a major consideration in the science of microclimatology. Geiger (1966) presents a fine discussion of the difficulties involved in measuring temperatures from the surface to a height of two meters.

Most of the temperature data which are available within the lowest two meters are termed "surface temperature." These so called surface temperatures are usually the air temperatures obtained in weather shelters at about eye level (shelter height). This height was selected as the level at which the chance influences of position on meteorological measurements were largely eliminated. Most meteorological networks throughout the world have adopted the temperatures monitored at shelter height as a standard for forecasting and climatological purposes. Although it is known that the temperature at this height may not always give a true indication of the temperature of the earth's surface or very near the surface, it is not critical for many uses. Often the actual temperature of the surface will differ by only a few degrees from the air temperature at shelter height. However, in instances of intense solar heating at the surface such as are encountered in deserts, and in instances of severe radiation cooling on clear nights with low wind speeds, the temperature difference between the surface and shelter height may be substantial. With a basic knowledge of micrometeorological processes, and information on prevailing meteorological conditions, a reasonable estimate of the temperature differences between shelter height and the surface may be made. For example, if one were to measure the temperature distribution from a snow surface to a height of two meters on a cold clear night with no wind, a temperature inversion of from 2 to 6C might be found due to radiation cooling of the snow surface. If the same temperature structure were monitored during the day with a moderate wind the inversion would be much reduced or even absent. The temperature at the snow surface would very likely be almost the same as at a height of two meters.

Extensive portions of the earth exist, notably in polar and mountainous regions, which are snow covered. Often these regions have a pronounced lack of temperature data from the surface to shelter height. This paucity of temperature information in the layer in which most life exists could be substantially decreased if the actual snow surface temperature could be conveniently monitored and related to temperatures at shelter height. With the development of radiation detectors which are able to remotely measure infrared radiation (thermal radiation) given off by all surfaces, a new tool has been made available for surface temperature measurement. Application of infrared radiation detectors (radiometers) to the problem of sparse temperature data in remote arctic and alpine environments may offer a workable solution. They may be incorporated into data acquisition systems in airplanes or satellites capable of rapidly monitoring large areas. In this manner increased surface temperature information might be obtained in otherwise inaccessible regions. Surface temperature data obtained by a system employing infrared radiometers are valuable for a number of reasons.

Surface temperature information is important in the study of the heat flux at the land-air and sea-air interfaces, as well as in the investigation of infrared radiation flux in the lower atmosphere. Surface temperature data have also found application in economic and military fields. New areas on the earth's surface, especially in polar regions, have been exploited for their petroleum wealth. Large sections of these lands lack population and thus, surface and near surface (shelter height) temperature information. Now that man has extended his activities into these regions such information has become an important consideration for movement of men and materials.

Surface temperature information might be of significant worth from a military point of view. Our nation often finds itself immersed in conflicts over all parts of the globe. Our combat forces must be prepared to fight in all types of environments from the equatorial latitudes to polar regimes. Surface temperature information in such areas may be difficult to obtain by conventional means with the presence of an enemy to consider, and yet may be essential for planning of tactical maneuvers.

The thermal agitation of the molecules in all materials causes the emission of electromagnetic energy (Figure 1.1). For objects at temperatures between -100C and 1000C, 80 per cent of this energy is in the infrared region between 1.8 and 40 microns. Because the physical laws of radiation emission are well known, and because it is now possible to use electro-optical techniques to measure this radiation, reliable non-contact measurements of the temperature of distant objects can readily be made. Most infrared radiometers analyze only that portion of the thermal radiation falling in approximately the 8 to 14 micron spectral region (Figure 1.2). This region of the infrared spectrum is termed the atmospheric infrared "window" because it is a range with comparatively minor absorption of radiant energy by water vapor and carbon dioxide. Although other narrower windows exist, the 8 to 14 micron bandwidth is most often preferred in radiometry due to the relatively abundant radiant energy available to activate sensory equipment.

1.2 Definition of the Problem

The basic aim of the research was to explore the feasibility of using an airborne infrared thermometer to monitor snow surface temperatures. In order to accurately determine surface temperature using an infrared radiometer, the emissivity of the surface must be known. The

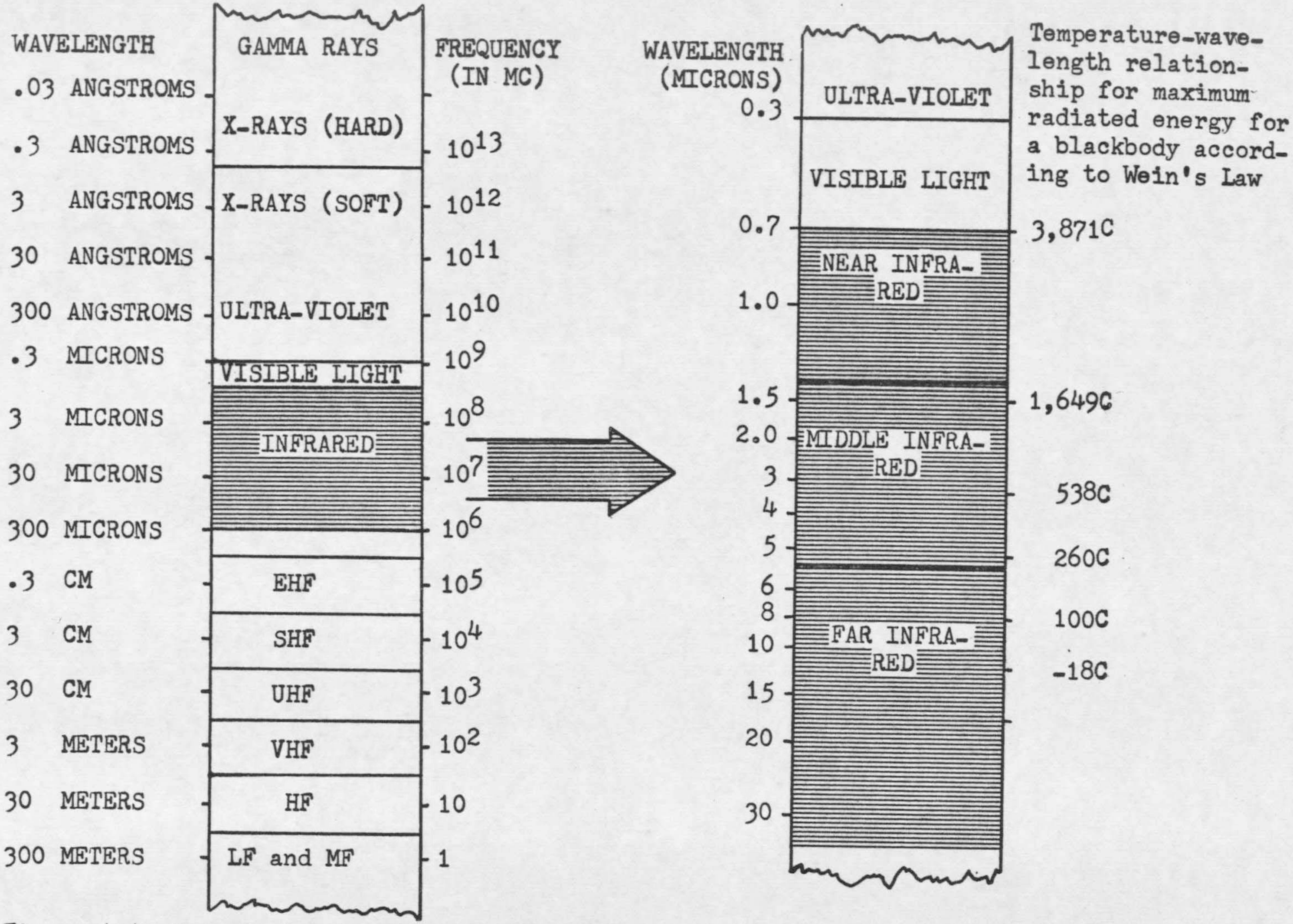

Figure 1.1 The electromagnetic spectrum and an expansion of the infrared region showing wavelength of maximum or peak emission for indicated temperatures.

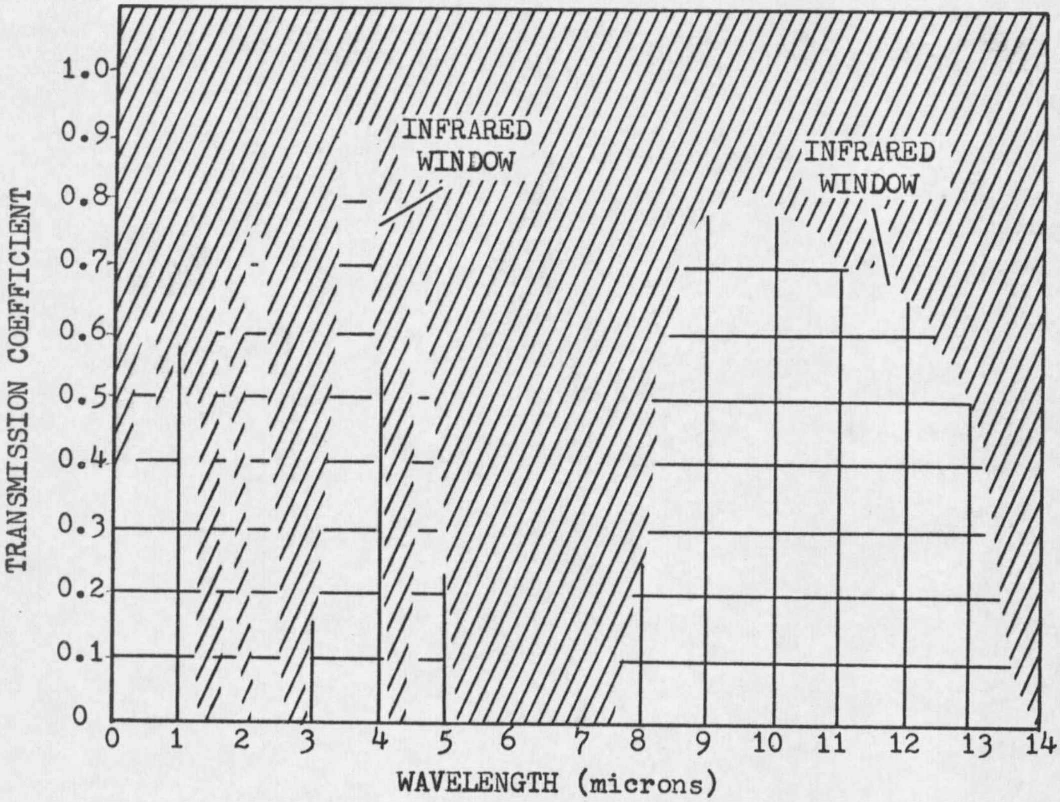

Figure 1.2 Spectral locations of atmospheric infrared "windows."

emissivity is defined as the ratio of the radiant power per unit area emitted by a surface to the radiant power emitted by a blackbody at the same temperature. A blackbody is a theoretical body which absorbs all radiation it intercepts, and emits the maximum radiation possible at every wavelength for its temperature. Some investigators, when analyzing infrared data, have assumed that earth surfaces radiate as a blackbody. In reality no naturally occurring surface is a perfect emitter in the 8 to 14 micron wavelength range. Emissivity is a function of both temperature and wavelength. Figure 1.3 demonstrates the effect of emissivity on surface temperature determinations using a radiometer which senses radiant energy in the 8 to 14 micron band. For any surface an emissivity over a portion of the spectrum (spectral emissivity) or over the entire spectrum (total emissivity) may be designated. For most natural surfaces the emissivity, whether it be total or spectral, remains relatively constant in the temperature range -40 to 100C (Kern, 1965). This is an important point for infrared thermometry, because the emissivity of a surface must remain invariant with respect to spatial and temporal variations in order that surface temperatures calculated from radiative measurements be accurate.

A search of the literature for a unique value of the emissivity of dry snow revealed conflicting and sometimes confusing data. Since the correct emissivity of snow is essential in determining actual snow

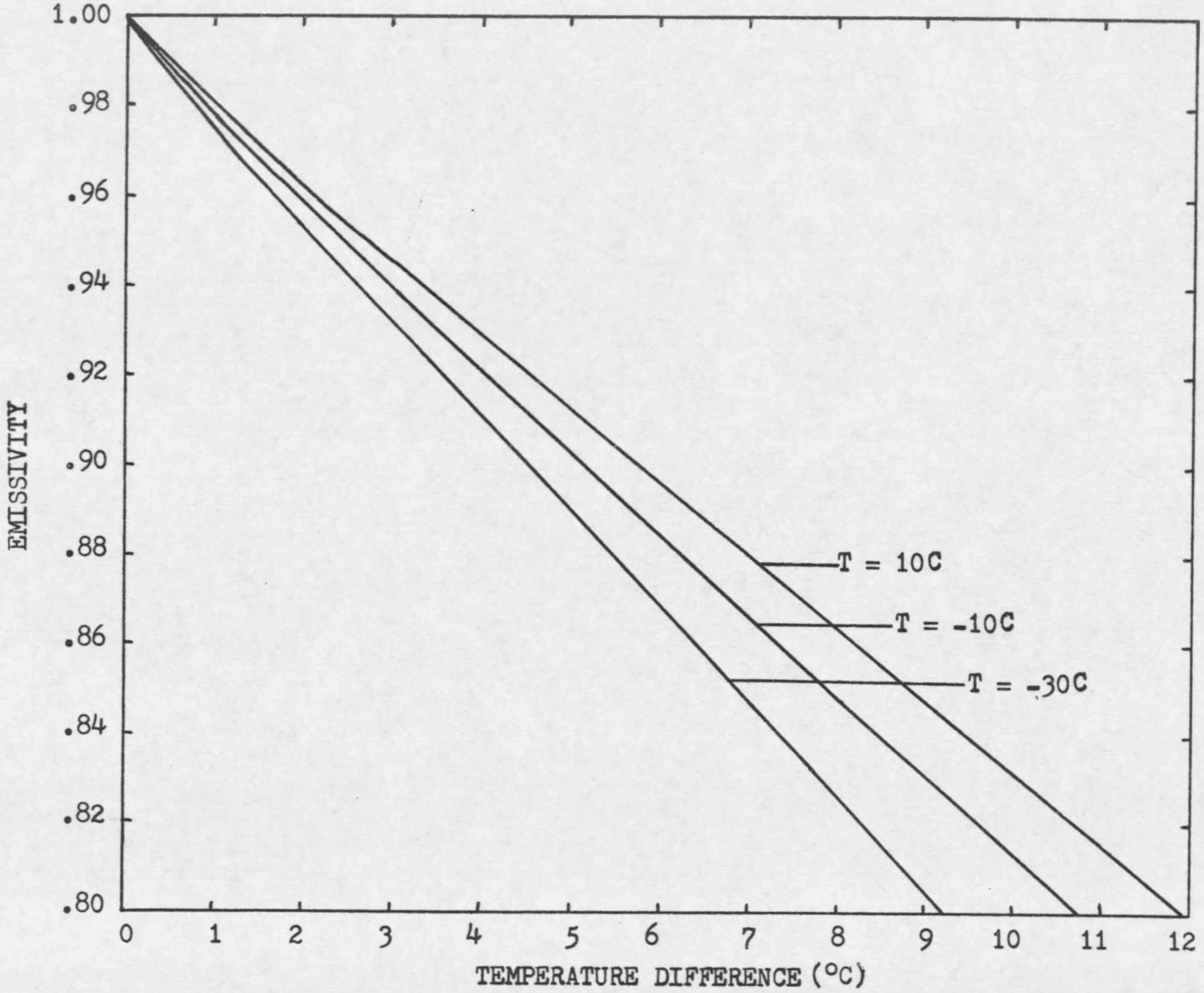

Figure 1.3 Temperature difference between the true surface temperature and the temperature indicated by a radiometer as a function of emissivity and surface temperature.

surface temperatures from radiometrically obtained data, it was decided that a basic goal of the research would be the determination of the emissivity of dry snow in the 8 to 14 micron wavelength region. To accomplish this an infrared radiometer manufactured by Barnes Engineering Company and an apparatus called an "emissivity box" were used.

Radiometric temperature measurements of surfaces having an emissivity near unity require little correction to obtain actual surface temperatures. Once snow and ice surfaces were found to possess a very high emissivity in the 8 to 14 micron interval, the study concentrated on determining the feasibility of using an airborne radiometer to monitor snow surface temperatures. Comparisons of radiometrically obtained snow surface temperatures and air temperatures at shelter level were made to determine if reliable estimates of shelter temperature could be derived from radiometric surface temperatures. Several case studies were made for varying meteorological conditions.

Radiometrically determined surface temperatures obtained from an aircraft are influenced by factors other than the temperature and the emissivity of the surface. The more important factors are reflected radiation from nearby objects, reflected sky radiation, reflected cloud radiation, and atmospheric attenuation in the intervening column of air between the sensor and the surface. Admittedly, these influences which are external to the surface under investigation are often assumed insignificant. However, if the magnitude of their effects is known, the error which they induce may be eliminated or at least estimated and the accuracy of the measurements thereby improved. For this reason the effect of reflected radiation and atmospheric absorption on radiometric temperature sensing was examined.

The primary goal of the research was to determine the feasibility of using an airborne radiometer to accurately monitor snow surface temperatures. In order to achieve this goal it was first necessary to determine the emissivity of snow in the 8 to 14 micron interval. Thus, field investigation was conducted in two stages. First, emissivity measurements were made of a large number of snow samples and an average emissivity computed. In the second stage several airborne flights were made over snowfields, and snow surface temperature gradients obtained with the radiometer were mapped. Radiometric snow surface temperatures obtained on these flights were compared with shelter level temperatures. The effect of reflected radiation and absorption on radiometric temperature sensing was also explored.

Chapter 2

SURVEY OF RECENT INFRARED TEMPERATURE SENSING INVESTIGATIONS AND ELEMENTARY RADIATION THEORY

2.1 General Remarks

During the early 1960s infrared technology for determining surface temperature advanced rapidly. This can be attributed largely to the wealth of infrared measurements which became available from the Tiros series of weather satellites.

Wark et al. (1962) analyzed the infrared data obtained from the Tiros II weather satellite. He arrived at a method for estimating infrared flux and surface temperatures from satellite infrared measurements. Corrections were made to account for filter characteristics of the radiometer and the absorption by water vapor and ozone in the atmosphere. The surface temperature which they correlated with the infrared radiation measured by the radiometer onboard the satellite was, in reality, the air temperature observed in instrument shelters.

Later, Kern (1963) discovered that the published surface temperatures derived from Tiros III infrared data were 10 to 20C too low. He found that the primary cause for the error was due to the variable emissivity of the surface. In order to better evaluate satellite infrared information Buettner and Kern (1965) designed and built a fieldworthy device to measure the infrared emissivities of natural surfaces. The emissivity values which they obtained have been largely verified by subsequent investigations: Lorenz (1966), Griggs (1968), and Dana (1969). For the purpose of illustrating the range of emissivities typically found, Table 2.1 presents some of the results obtained by Buettner and Kern and Lorenz.

The feasibility of using an airborne radiometer to measure surface temperature variation has been explored by several authors including Lenschow and Dutton (1964), Fujita et al. (1968), and Holmes (1968). In each case the emissivity of the surface was taken to be very near unity. Implicit in this is the assumption of a small range of emissivity values for natural surfaces. The error which this assumption produces was not critical for their purposes since relative temperature differences was the object of their efforts. The emissivity measurements made by Griggs (1968) of some natural surfaces were accomplished from an airborne platform. His treatment of the errors induced by the intervening atmosphere and for sunlight, skylight, and aircraft radiation are noteworthy.

Conway and Van Bavel (1967) and Idso and Jackson (1968) have probed the influence which fluctuations in sky radiant emittance exerts on radiometrically-determined surface temperatures. The conclusion reached by Idso and Jackson was that the error resulting from neglecting variations in sky radiant emittance is negligible except for very precise radiometry.

Infrared temperature sensing of ice and snow surfaces has received

Table 2.1 Normal emissivities of natural surfaces in the atmospheric infrared window between 8 and 14 microns.

Surface	Emissivity	Source
Granite, rough side	0.898	Buettner and Kern
Basalt, rough side, shiny	0.934	Buettner and Kern
Dunite, rough side	0.892	Buettner and Kern
Silicon sandstone, rough side	0.935	Buettner and Kern
Dolomite, rough side	0.958	Buettner and Kern
Dolomite gravel, 0.5 cm rocks	0.959	Buettner and Kern
Sand, quartz large grain	0.914	Buettner and Kern
Sand, quartz large grain, wet with water (nearly saturated)	0.936	Buettner and Kern
Sand, Monterey, quartz small grain	0.928	Buettner and Kern
Concrete walkway, dry	0.966	Buettner and Kern
Asphalt paving	0.956	Buettner and Kern
Water, pure	0.993	Buettner and Kern
Water plus thin film of petroleum oil	0.972	Buettner and Kern
Sand as used for mixing mortar	0.938	Lorenz
Slab of concrete	0.942	Lorenz
Coarse gravel, smooth round pebbles	0.943	Lorenz
Brick roof tile, old	0.950	Lorenz
Fine basaltic gravel with jagged edges	0.952	Lorenz
Asphalt, old road surface	0.955	Lorenz
Lawn, very dense and well kept	0.973	Lorenz

little attention. Miller (1963) reported results of a program which involved measuring the surface temperature of ice and snow surfaces over the Greenland ice cap by means of airborne radiometry. Combs et al. (1964) presents results of flights over Arctic terrain, some of which was covered by ice and snow. Griggs (1968) calculated the emissivity of a melting snow surface using an airborne radiometer. The air temperature over the snow surface was above freezing suggesting that the emissivity value obtained was probably for a thin film of liquid water on the snow surface.

To this writer's knowledge reports on infrared temperature sensing programs over snow and ice surfaces have not been widely published; inquiries to the Infrared Information Analysis Center at the University of Michigan, considered by many to be the clearing house for infrared sensing information, have revealed a definite lack of emissivity information for snow surfaces. Most investigations in this realm of radiometry have assumed very nearly unit emissivities for these types of surfaces. As will be shown, however, the validity of this assumption may seem questionable in light of the range of published values for the emissivity of snow and ice given in section 2.3.

Before commencing this discussion it is helpful to review some fundamental concepts in radiation theory applicable to the infrared wavelengths utilized.

2.2 Elementary Radiation Theory and Definition of Terms

In order to facilitate understanding of subsequent derivations, a number of terms frequently encountered are presented and defined in Table 2.2. For a more detailed account of infrared technology than will be given here, see Wolfe (1965).

Radiant energy is energy in transit. Radiant energy, when encountering a medium other than a vacuum, may be either transmitted, reflected, absorbed, or undergo a combination of these three processes. The degree to which any of the three occur is highly dependent on wavelength. This relationship may be expressed by

$$a_\lambda + r_\lambda + t_\lambda = 1 \qquad (2.1)$$

where a_λ is the absorptivity at wavelength λ, r_λ is the reflectivity at wavelength λ, and t_λ is the transmissivity at wavelength λ. A body which has an absorptivity equal to unity at all wavelengths is termed a blackbody. This stipulation of unit absorptivity requires that the reflectivity and the transmissivity equal zero. Perfect blackbodies do not exist in nature, but they are often closely approximated by natural surfaces at infrared wavelengths.

A further development of radiation theory asserts that under the condition of thermodynamic equilibrium, the emissivity for a given wavelength is equal to the absorptivity at the same wavelength. This law, known as Kirchoff's Law, can be stated in the form

Table 2.2 Definition of radiation terminology.

Term	Units	Definition
Radiant power	watts	The radiant energy emitted by a surface per unit time.
Spectral radiant power	watts/micron	The radiant power emitted by a surface within a given spectral range.
Radiant intensity	watts/steradian	The radiant power emitted by a source per unit solid angle.
Spectral radiant intensity	watts/ster./micron	The radiant intensity considered over a given spectral range.
Radiant emittance	watts/m^2	The radiant power emitted per unit area by a source into a hemisphere.
Spectral radiant emittance	watts/m^2/micron	The radiant emittance over a given spectral range.
Radiance	watts/m^2/steradian	The radiant power emitted by a source per unit solid angle per unit projected area.
Spectral radiance	watts/m^2/ster./micron	The radiance considered over a given spectral range.
Reflectivity	dimensionless	The fraction of radiant power incident on a surface which is reflected or back scattered.
Absorptivity	dimensionless	The fraction of radiant power absorbed by a medium.
Transmissivity	dimensionless	The fraction of radiant power transmitted by a medium.
Emissivity	dimensionless	The ratio of the radiant emittance of a source to the radiant emittance of an ideal blackbody radiator at the same temperature.
Spectral emissivity	dimensionless	The emissivity of a source considered over a given spectral range.

$$a_\lambda = \epsilon_\lambda \tag{2.2}$$

If we now consider the body to have zero transmissivity (i.e. it is opaque to radiation of a given wavelength and substitute Eq. 2.2 into Eq. 2.1), we arrive at

$$\epsilon_\lambda = 1 - r_\lambda = a_\lambda \tag{2.3}$$

which declares that the emissivity at a specified wavelength is equal to one minus the reflectivity at the same wavelength. It should be remembered that this relationship is true only for opaque bodies. The restriction to opaque bodies is not as severe as it might seem. Gubareff _et al_. (1960) states that most materials are opaque at infrared wavelengths.

The spectral radiant emittance, $B^*(\lambda,T)$, of a body at temperature T is given by Planck's Law of blackbody radiation

$$B^*(\lambda,T) = C_1 \lambda^{-5}(\exp(C_2/\lambda T) - 1)^{-1} \quad (\text{watts/cm}^2\text{/micron}) \tag{2.4}$$

where $C_1 = 3.7405 \times 10^4$ (watts-micron^4/cm^2)

$C_2 = 1.43879$ (microns-$^\circ$K)

λ = wavelength (microns)

Figure 2.1 presents several representative curves of spectral radiant emittance into a hemisphere versus wavelength derived by evaluating the Planck function for the indicated temperatures which are typical of

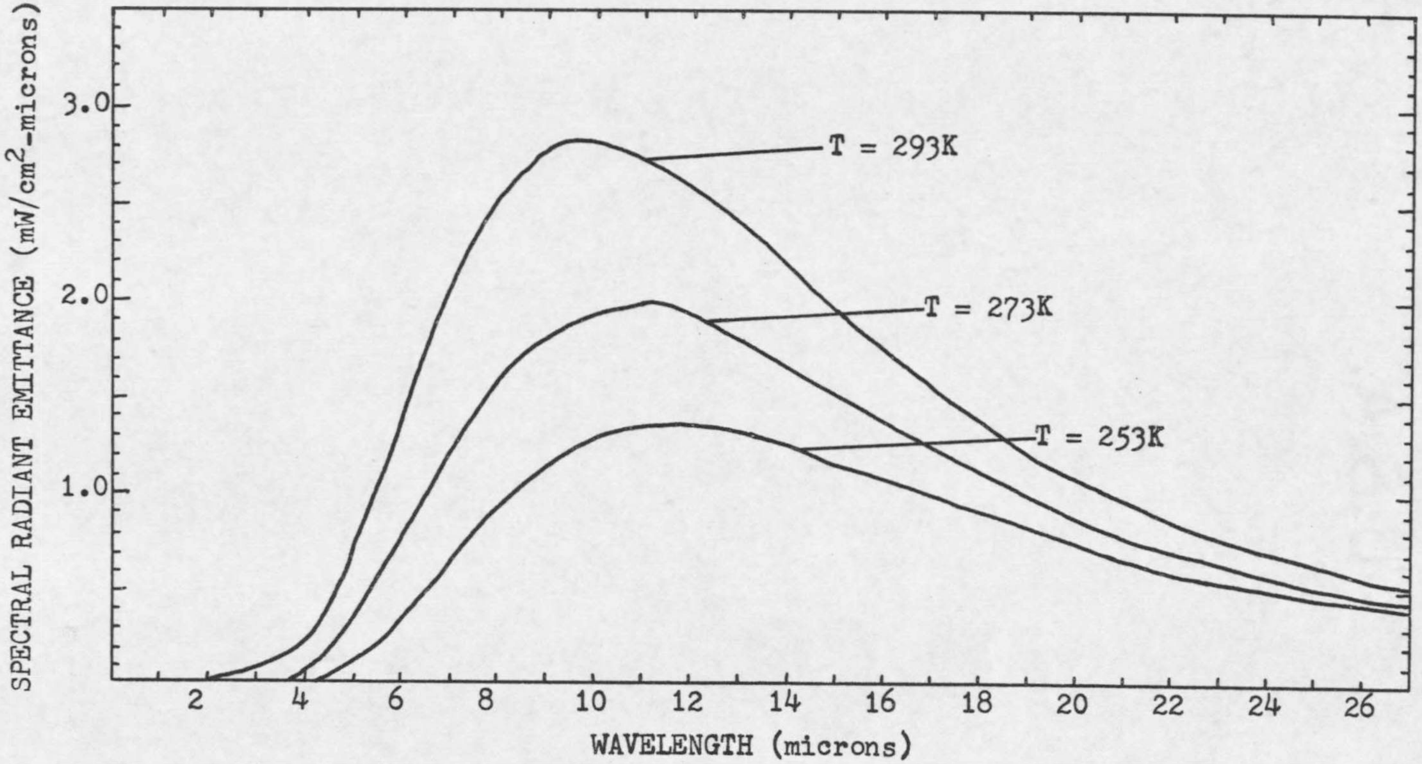

Figure 2.1 Blackbody radiation curves for the temperature range commonly experienced by natural surfaces.

terrestrial surfaces.

If the spectral radiant emittance of Planck's Law is integrated over all wavelengths, the Stefan-Boltzmann Law results. This law relates the total radiant emittance for a blackbody, W_{bb}, to the fourth power of the absolute temperature. In mathematical notation this law is expressed as

$$W_{bb} = \sigma T^4 \tag{2.5}$$

where σ is the Stefan-Boltzmann constant having a value of 5.6698×10^{-12} watts cm^{-2} $^{o}K^{-4}$ as established by the U.S. National Academy of Sciences and the Canadian National Research Council (Landsberg et al., 1970).

To obtain the wavelength of maximum intensity for blackbody radiation, Planck's Law is differentiated with respect to wavelength and solved for wavelength. This produces Wein's Displacement Law

$$\lambda_{max} = \frac{2897}{T} \quad (\text{microns-}^{o}\text{K}) \tag{2.6}$$

From this law it is obvious that the wavelength of maximum intensity, λ_{max}, increases with decreasing temperature. In the range of temperatures commonly experienced by terrestrial surfaces, the wavelength of maximum intensity lies within the atmospheric infrared window between 8 and 14 microns.

If the source is not a perfect blackbody (a "graybody") the total radiant emittance, W, from that source is described by

$$W = \epsilon_t \sigma T^4 \tag{2.7}$$

where ϵ_t now becomes the emissivity averaged over all wavelengths. Equation 2.7 is a more accurate representation of the condition which exists in nature than Eq. 2.5, since all natural surfaces can be considered graybodies to varying extents. The total radiant emittance from natural surfaces must necessarily be less than the total radiant emittance of a blackbody at the same absolute temperature because the value of ϵ_t is less than or equal to 1.0.

To obtain the radiance from a surface, Lambert's Law is applied. This law states that the radiant intensity (flux per unit solid angle) emitted in any direction from a unit radiating surface varies as the cosine of the angle between the normal to the surface and the direction of radiation. Expressed another way, the emitted radiation from a blackbody has no preferred direction of propagation. If, however, the surface acts approximately as a perfectly diffuse radiator, Lambert's Law is also valid. Such is the case for many natural surfaces, and in particular snow surfaces. The radiance, N_{bb}, for a perfect blackbody is given by

$$N_{bb} = \frac{W_{bb}}{\pi} = \frac{\sigma T^4}{\pi} \tag{2.8}$$

and the radiance, N, for a graybody by

$$N = \frac{W}{\pi} = \frac{\epsilon_t \sigma T^4}{\pi} \tag{2.9}$$

At this point the total average emissivity, ϵ_t, can be defined as

$$\epsilon_t = \frac{N}{N_{bb}} \tag{2.10}$$

where both the blackbody radiation source and the graybody radiation source are at the same temperature.

With the preceding radiation theory in mind, the emissivity of a snow surface can be developed.

2.3 Spectral Emissivity and Total Emissivity of Snow

Many commercially available infrared radiometers do not measure radiation over all infrared wavelengths. Rather, through an optical filtering system, the radiation accepted by the radiometer is confined to a limited spectral region coincident with the atmospheric window portion of the spectrum. Emissivities of surfaces determined by employing such radiometers are thus spectral emissivities. Further, reported emissivities frequently are restricted to orientations normal to the surface giving rise to what is termed the spectral normal emissivity of the surface, ϵ_s, weighted by the filer response of the radiometer, $q(\lambda)$. ϵ_s is defined through the use of an equation

$$\epsilon_s = \frac{\int_0^\infty q(\lambda)\, E(\lambda, T_s)\, d\lambda}{\int_0^\infty q(\lambda) B^*(\lambda, T_s)\, d\lambda} \tag{2.11}$$

where $E(\lambda, T_s)$ is the spectral radiant emittance of the gray surface at temperature T_s, $B^*(\lambda, T_s)$ is the spectral radiant emittance of a blackbody at temperature T_s, and $q(\lambda)$ is the filter function of the radiometer specifying the spectral range of the radiometer.

The spectral emissivity, ϵ_s, of Eq.2.11, may be less than, equal to, or greater than the total emissivity, ϵ_t, of Eq. 2.10. This may happen because emissivity is a function of wavelength as well as temperature and is not constant over the entire infrared region of the spectrum.

Both spectral and total emissivities have been published for snow and ice surfaces, although at times the distinction as to which was meant is not made clear. Unless otherwise noted, all emissivities mentioned in this work are spectral emissivities valid in the 8 to 14 micron bandwidth.

Buettner and Kern (1965) reported that Falckenberg (1928) arrived at an emissivity for snow equal to 0.995 which was very nearly the same as the emissivity calculated by Griggs (1968) for a melting snow surface. As previously noted, emissivity values for melting snow are, in all likelihood, emissivities calculated for a thin film of liquid water on the snow surface. McAlister (1964) has shown that when a substance such as water covers a surface to depths of 0.02 mm an essentially new radiating surface is apparent. The new effective surface may mask the true radiative properties of the underlying surface.

Weingeroff (1931) conducted a study of the infrared reflectivity of water and ice. His results, as reported by Buettner and Kern (1965), are presented in the curves of Figure 2.2.

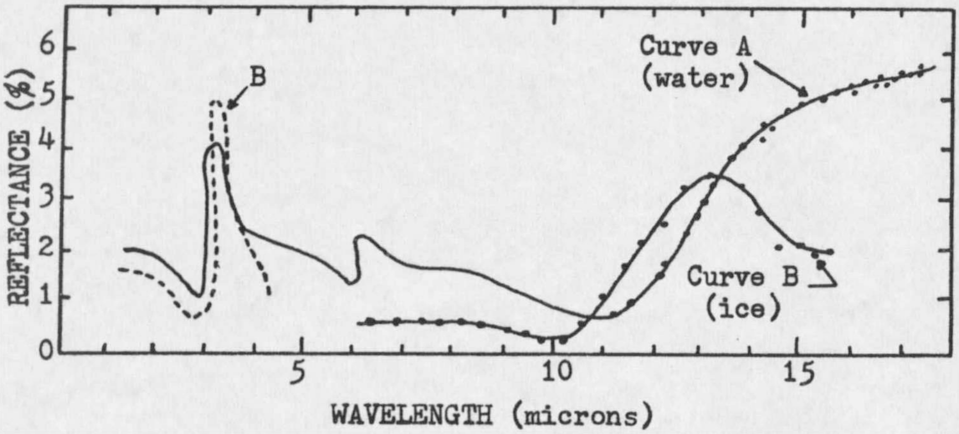

Figure 2.2 Vertical reflectance curves for water (Curve A), and for a smooth ice surface (Curve B) due to Weingeroff (1931) as reported by Buettner and Kern (1965). Curve B is only relative due to the formation of frost on the surface.

Applying the results of Eq. 2.3 and extending the emissivity and reflectivity terms to denote an average over the interval 8 to 14 microns, we arrive at $\epsilon_s = 1 - r_s$. The emissivity for ice which is shown by Weingeroff's data according to this relation is approximately 0.98 for the 8 to 14 micron window region. The peak in reflectivity seen at 13 microns makes it difficult to estimate the emissivity of dry snow in the window region without actual measurements.

Dunkle et al. (1955) presents a total longwave emissivity of 0.82 for new snow, similar in size to frost crystals, for a temperature range of 15.0 to 19.5F. This value is often quoted in the literature. In the same report by Dunkle, a total emissivity for granular snow (approximately 1/32 of an inch in diameter) is listed as 0.89 for a temperature range of 13.0 to 21.0F, while an emissivity of 0.95 is reported for ice crushed into crystals slightly larger than the granular snow. Ice ground in a blender was found to exhibit a total emissivity of 0.81. The total emissivity of a crushed ice sample was found to be a function of temperature as the sample was warmed to the melting point from 22.5F. The emissivity varied from 0.87 at the lower temperature to 0.95 at 32F. Dunkle concluded that the emissivity variation between snow and ice surfaces is a function of particle size and surface roughness and is imperfectly understood.

The emissivity for a snow surface in Greenland, determined from data presented by Miller (1963), is calculated to be between 0.43 and 0.66. Cirrus clouds composed of ice crystals have been found to have emissivities in the 8 to 13 micron region which vary from 0.05 to 1.00 (Valovcin, 1968). Gubareff et al. (1960) presents a total emissivity for rime ice equal to 0.985. Geiger (1966), Gates (1961), and the U.S. Army Corps of Engineers Snow Hydrology report (1956) suggest that snow and ice are nearly perfect blackbody radiators at infrared wavelengths.

From the previously cited literature it is evident that significant discrepancies exist concerning the emissivity of snow in its diverse forms. Clarification of these conflicting data, at least for the spectral band 8 to 14 microns, is attempted in Chapter 4.

Before proceeding to report on the emissivity investigations undertaken by the writer, the characteristics of the radiometer which was utilized for the investigation are discussed.

Chapter 3

DESCRIPTION OF RADIOMETER

3.1 General Description of Radiometer and Recorder

The instrument used for all radiometric measurements in this investigation was a Model-A Barnes IT-3 Infrared Thermometer manufactured by the instrument division of Barnes Engineering Company. This model has a capacity for measurements in the temperature range -40 to 60C. It consists of a thermistor-bolometer detector, chopper, and preamplifier in a sensing head which is connected to a compact, portable electronic console containing a post amplifier and the power supply.

The radiant energy is collected and filtered by the optical system in the sensing head. A germanium filter focuses the radiation on the thermistor-bolometer detector. Indium antimonide provides the filter material for the short wavelength cutoff at eight microns and a Kodak Irtran-2 filter provides the long wavelength cutoff at 14 microns. The incoming radiation from the target is modulated at a frequency of 90 cps by a gold plated chopper. As the chopper rotates, the detector alternately compares the target radiation to radiation from an internal, temperature controlled blackbody reference cavity. The result is the generation of an a.c. signal proportional to the energy difference between the target radiance and the radiance from the internal cavity. The a.c. signal is preamplified and transmitted to an electronic console where it is further amplified, demodulated, and rectified to provide a d.c. output which drives a meter circuit and recorder output circuit. Since the radiance from the target is determined by its temperature, the radiometer output can be calibrated in terms of target temperature if the target is radiating as a blackbody.

The field of view of the radiometer is three degrees focused at infinity. The size of the viewing area is reported by the manufacturer to be a one inch square at one foot and a 57 foot square at 1000 feet. Investigations by Dana (1969) for a Barnes model PRT-5 with similar sensing head revealed that the radiometer actually "saw" radially outward a considerably greater distance than advertised by the marketing firm. From his evidence it might be concluded that where knowledge of the area viewed by the radiometer is critical, tests should be conducted to verify the dimensions of the effective viewing area.

The absolute accuracy as stated by the manufacturer of the infrared thermometer is ±2C above 0C and ±4C below 0C. The advertised resolution is 0.5C above 0C and 1C below 0C. These accuracy figures are specified for a target of unit emissivity in the spectral range of the radiometer. During the calibration procedures for the radiometer reported later in this chapter, the accuracy figures stated above were substantiated by actual measurements.

The IT-3 is equipped with a selector switch which provides the user access to either a "fast" response or a "slow" response. In the "fast" position, 50 milliseconds are required to achieve 63 per cent of full response to a step change in input signal, while in the "slow" position the response time is 500 milliseconds. The slow mode has the advantage of reduced noise and greater resolution. For the purposes of this research the slow mode was found to result in a superior quality of data obtained on a recorder.

A Leeds and Northrup Speedomax H strip chart recorder was utilized with a full scale range of ten millivolts. Advertised accuracy for this recorder is ± 0.3 per cent of electrical span. The span step-response-time rating is one second for a full scale deflection. A record is obtained using a multi-point print wheel rather than a continually recording pen with the print time per point equal to 1.2 seconds. The 1.2 second print cycle permits an accurate record well within the response time of the recorder for instantaneous fluctuations in signal.

The d.c. output of the infrared thermometer (IRT) is 50 millivolts full scale adjustable. Since the 50 millivolt output for which the IRT was factory-calibrated against blackbody reference sources was not commensurate with the Leeds and Northrup recorder's capability, it was adjusted to output a signal in the range 0 to 10 millivolts full scale. This adjustment necessitated a new calibration to correct for the change in the range of the IRT output. To accomplish this a blackbody calibration chamber was designed and built. Calibration procedures and results are given in section 3.3.

3.2 Spectral Response of the IT-3

The precise filter transmission characteristics for the radiometer were not available from the manufacturer at the time data compilation and synthesis for this study was done. Figure 3.1 gives a transmission curve reported by Dana (1969) for a Barnes PRT-5 which is believed to be the same as for the IT-3 Model-A. It is presented here to provide an example of the mechanics involved in computing the radiance effective at the sensor. As is readily seen from Figure 3.1 the filters actually allow infrared radiation outside of the advertised 8 to 14 micron band-pass. The total spectral response, $q(\lambda)$, is thus the transmission over the range from about 7.4 to 16.7 microns with a minor response near 19 microns. Therefore, to describe the radiant energy which the IT-3 senses, the blackbody spectral emittance curve for a particular temperature is multiplied point by point by the transmission curve of Figure 3.1. In Figure 3.2 this process has been done for a temperature of 253K. The area under the dashed line represents that portion of the radiant emittance from a blackbody sensed by the IT-3.

Radiant energy emitted by a graybody is often referred to as blackbody radiance. The concept of blackbody radiance of a graybody is interpreted to mean the temperature at which a blackbody would radiate in order to produce the same amount of radiant energy as the graybody. An expression for this quantity may be derived by integrating a form of Planck's Law which is slightly different than Eq. 2.4. The altered form

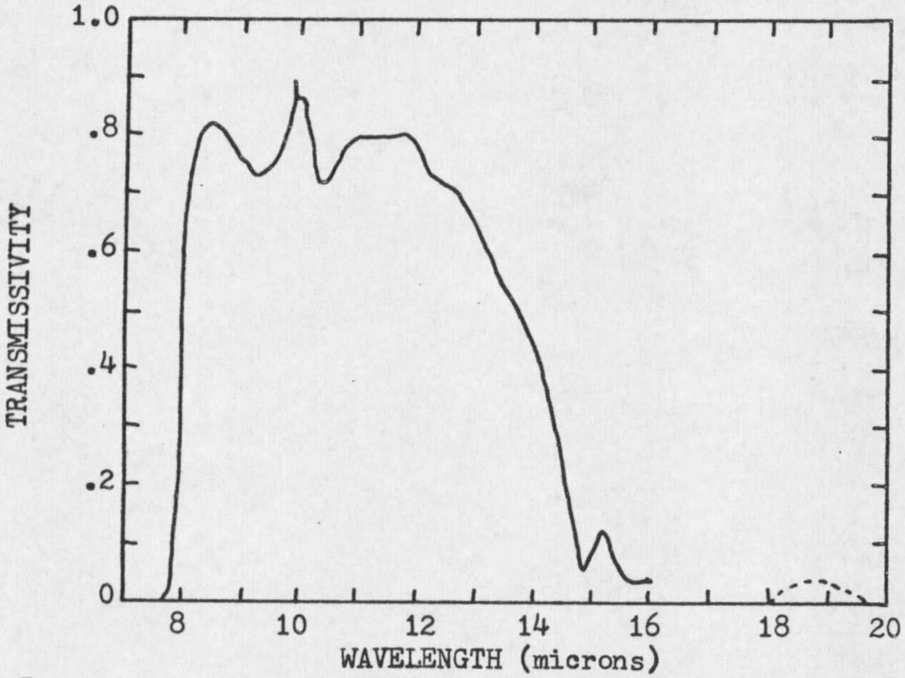

Figure 3.1 Transmission curve of PRT-5 which is similar to that of the IT-3 (after Dana, 1969).

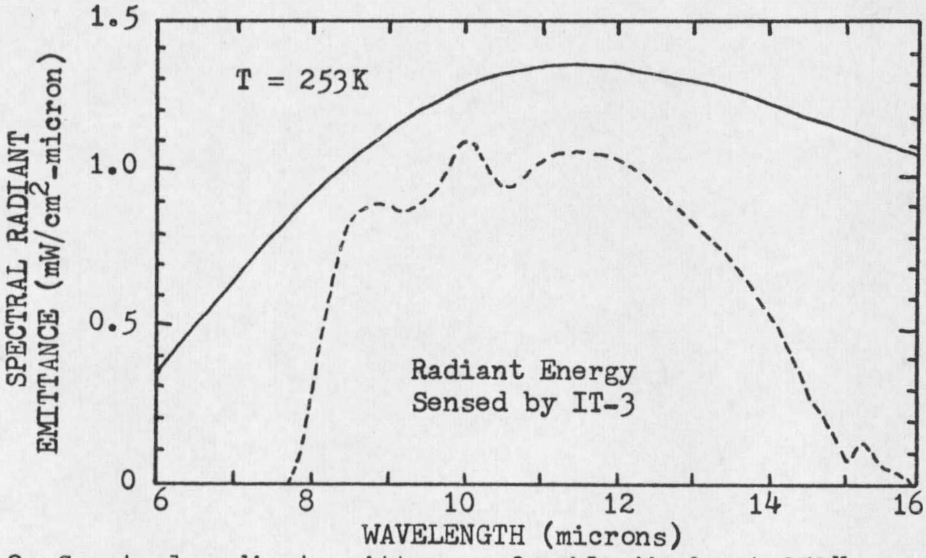

Figure 3.2 Spectral radiant emittance of a blackbody at 253K sensed by IT-3. Dashed curve is formed by multiplying the blackbody curve by the transmission curve of Figure 3.1.

of Planck's Law to be integrated is

$$B(\lambda,T) = 2hc^2 \lambda^{-5} (\exp(hc/k\lambda T) - 1)^{-1} \quad \text{(watts/micron/cm}^2\text{/steradian)} \tag{3.1}$$

where h = Planck's constant
c = velocity of light
λ = wavelength
k = Boltzmann constant
T = temperature in degrees Kelvin

The total radiance of a blackbody at temperature T can now be expressed by integrating Eq. 3.1 over all wavelengths

$$\int_0^\infty B(\lambda,T)\, d\lambda \qquad \text{(watts/cm}^2\text{/steradian)} \tag{3.2}$$

The effective blackbody radiance, B(T), of a blackbody entirely filling the field of view of the IRT is the blackbody radiance weighted by the spectral response $q(\lambda)$ of the IRT. It is given by

$$B(T) = \int_0^\infty q(\lambda)\, B(\lambda,T)\, d\lambda \quad \text{(watts/cm}^2\text{/steradian)} \tag{3.3}$$

Numerical integration of Eq. 3.3 was done using a computer, and the results were furnished by the manufacturer. Figure 3.3 is a curve of B(T) versus temperature for the IT-3 plotted from data supplied by the Barnes Engineering Company. Emissivity calculations for snow surfaces were computed using radiance values from this curve.

The IT-3 was designed for extensive use in the field of earth sciences, and the Model-A version was designed for measurements at relatively low terrestrial temperatures. The environment in which many

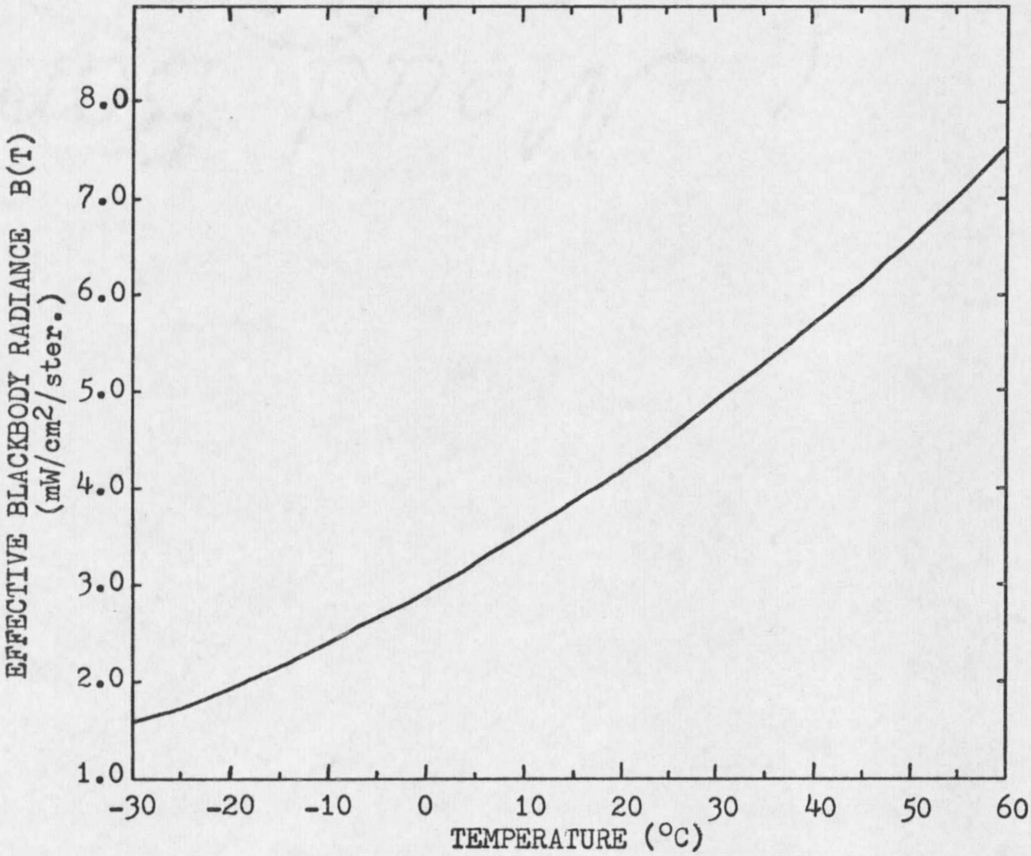

Figure 3.3 Effective blackbody radiance B(T) versus temperature for the Barnes IT-3.

measurements are made makes it imperative to be able to "look" through an intervening column of atmospheric constituents, both horizontally and vertically. If there were strong absorption (and correspondingly, strong emission) bands in the atmosphere, serious errors would be expected in radiometric measurements. However, as mentioned earlier, the existence of an infrared window in which there is relatively little absorption provides a solution to this problem. By designing the filter system of the radiometer to coincide with the infrared window region, absorption effects are minimized.

Figure 3.4 presents the infrared transmission characteristics of the earth's atmosphere looking vertically for typical concentrations of water vapor, carbon dioxide, and ozone--the three gases which primarily affect the absorption spectra at infrared wavelengths. It is easily seen that in the 8 to 14 micron spectral region of the IT-3, there is relatively little absorption except at 9.6 and 9.9 microns. Here, strong absorption exists due to the influence of the ozone vibrational band. If measurements are made at low levels in the atmosphere, the influence of the absorption band of ozone is of minor importance. In conjunction with the highly transparent regions from 8 to 14 microns it may be noted from Figure 2.1 that this particular range is also the region of peak thermal radiation.

The preceding discussion shows that the spectral bandpass of the IT-3 represents an optimum viewing interval for radiometric measurements,

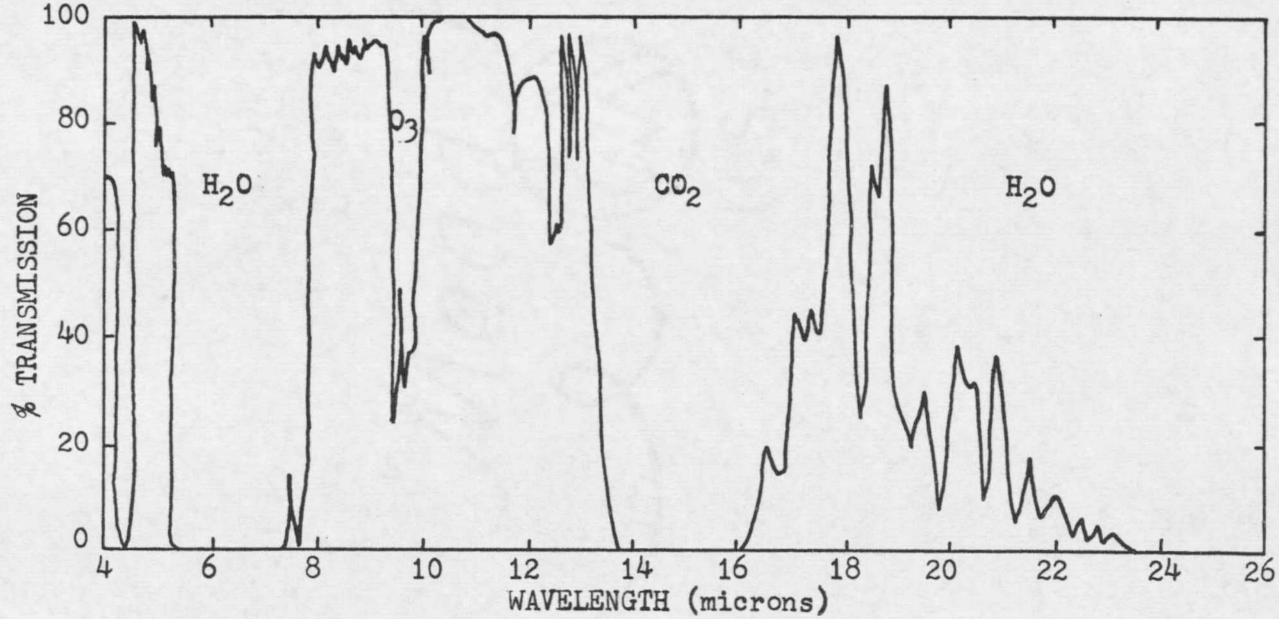

Figure 3.4 Transmission characteristics of the atmosphere for typical concentrations of water vapor, carbon dioxide, and ozone (after Gates, 1962).

especially for low temperature environments near the earth's surface.

3.3 Calibration of the Radiometer

Calibration procedures were carried out in an effort to obtain a stable curve of blackbody temperature versus millivolts output on the Leeds and Northrup recorder. At the same time the accuracy of the instrument was investigated and compared against factory specifications.

The basic technique in calibrating the infrared thermometer was to construct a blackbody and vary its temperature while tabulating the recorder output. The temperature of the blackbody needed to be uniform at the time readings were taken. This necessitated a calibration chamber with considerable thermal mass. To further complicate matters, temperatures below freezing were required.

The calibration chamber which was designed and built consisted of a high quality blackbody cavity housed in a cylindrical aluminum container (Figure 3.5) around which a liquid could be circulated to produce the variable temperatures needed. The blackbody cavity was constructed of two aluminum cones fastened base to base. One end was cut away to provide an aperture for viewing with the IRT. The interior of the cones was painted with Parsons Black Optical Paint. This is a special paint which possesses the property of an emissivity of 0.985 at infrared wavelengths.

The blackbody cavity was placed in a stirred bath of either ethylene glycol and water or water alone depending on the temperature

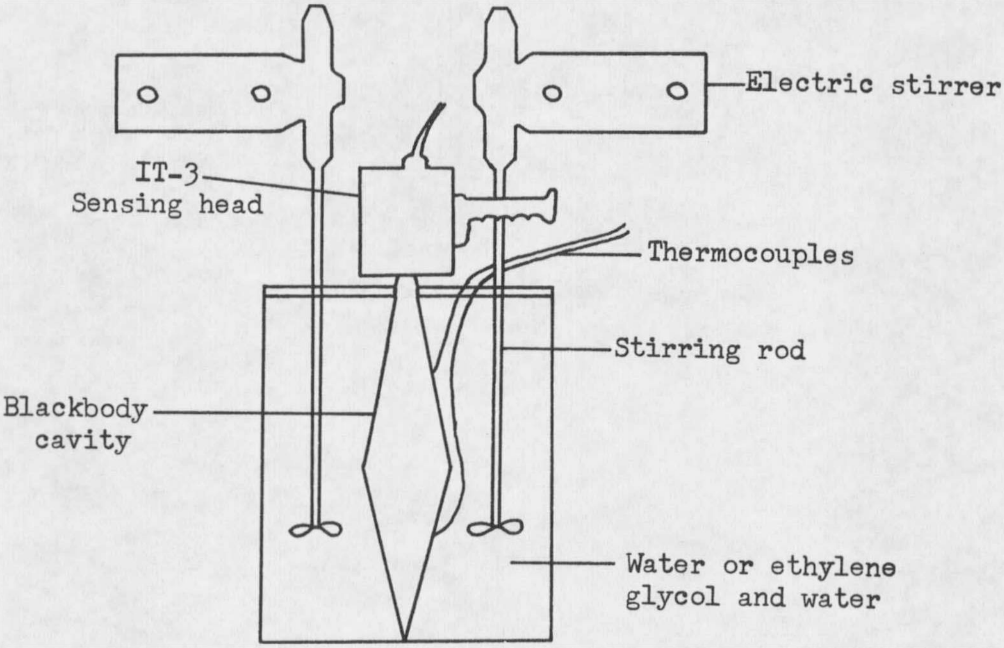

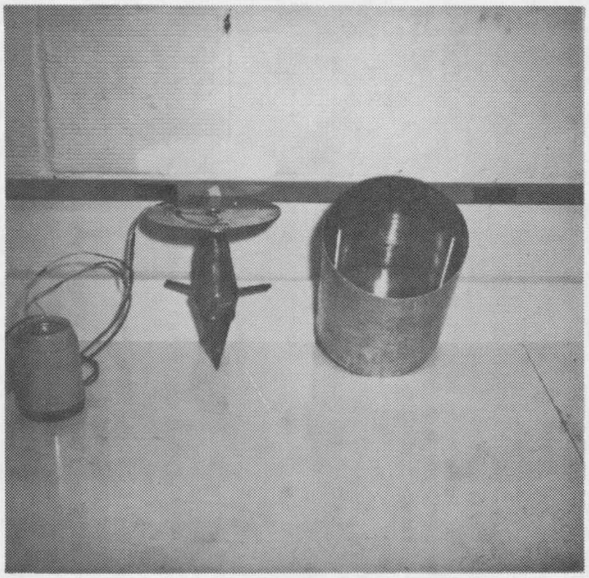

Figure 3.5 Upper--Diagram of blackbody calibration chamber.
Lower--Photograph of the blackbody cavity and its housing.

range for which the calibration was desired. The ethylene glycol and water solution was prepared in proportions of 2:1 respectively, to prevent a slush from forming at low temperatures. Two copper-constantan thermocouples were fixed to the exterior of the blackbody cavity to monitor its temperature. The temperature was varied slowly in order to eliminate temperature gradients through the aluminum shell of the cavity.

The temperature of the blackbody chamber was held uniform to within 0.1C through the use of electric stirrers. Calibration from 22C to -26C was accomplished by installing the blackbody apparatus in the nucleation chamber of a Bigg-Warner ice nuclei counter (Figure 3.6). The temperature of the chamber was reduced from room temperature to -26C and then allowed to warm to room temperature again. Temperature readings were taken continually both in the cooling and warming phases. Calibration from 22C to 60C was done by circulating hot tap water around the cavity while allowing it to cool slowly to room temperature (Figure 3.7). Thus, temperatures were recorded only for the cooling phase.

Five calibration runs were made in the lower temperature range while three were made in the higher range. The reason for the reduced number of runs in the higher temperature range was the excellent agreement in results from run to run.

The curve of Figure 3.8 was developed from the calibration procedures outlined. It is a mean curve derived from the individual

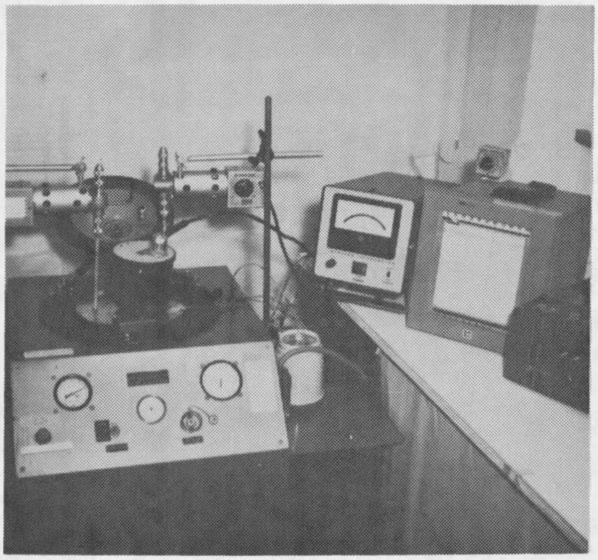

Figure 3.6 Calibration setup for the low temperature range.

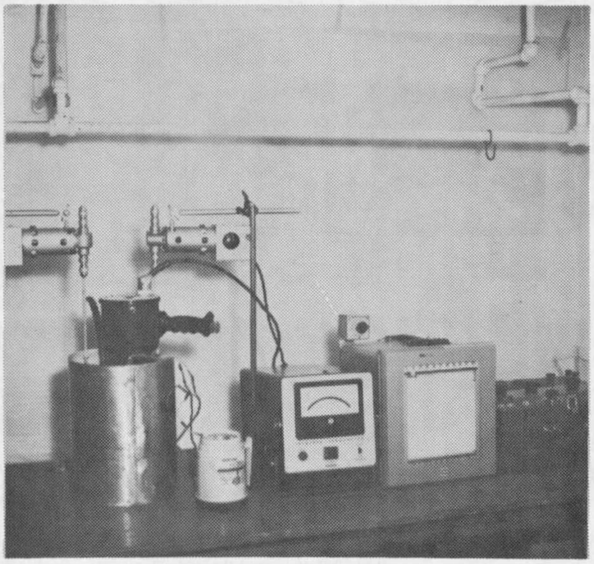

Figure 3.7 Calibration setup for the high temperature range.

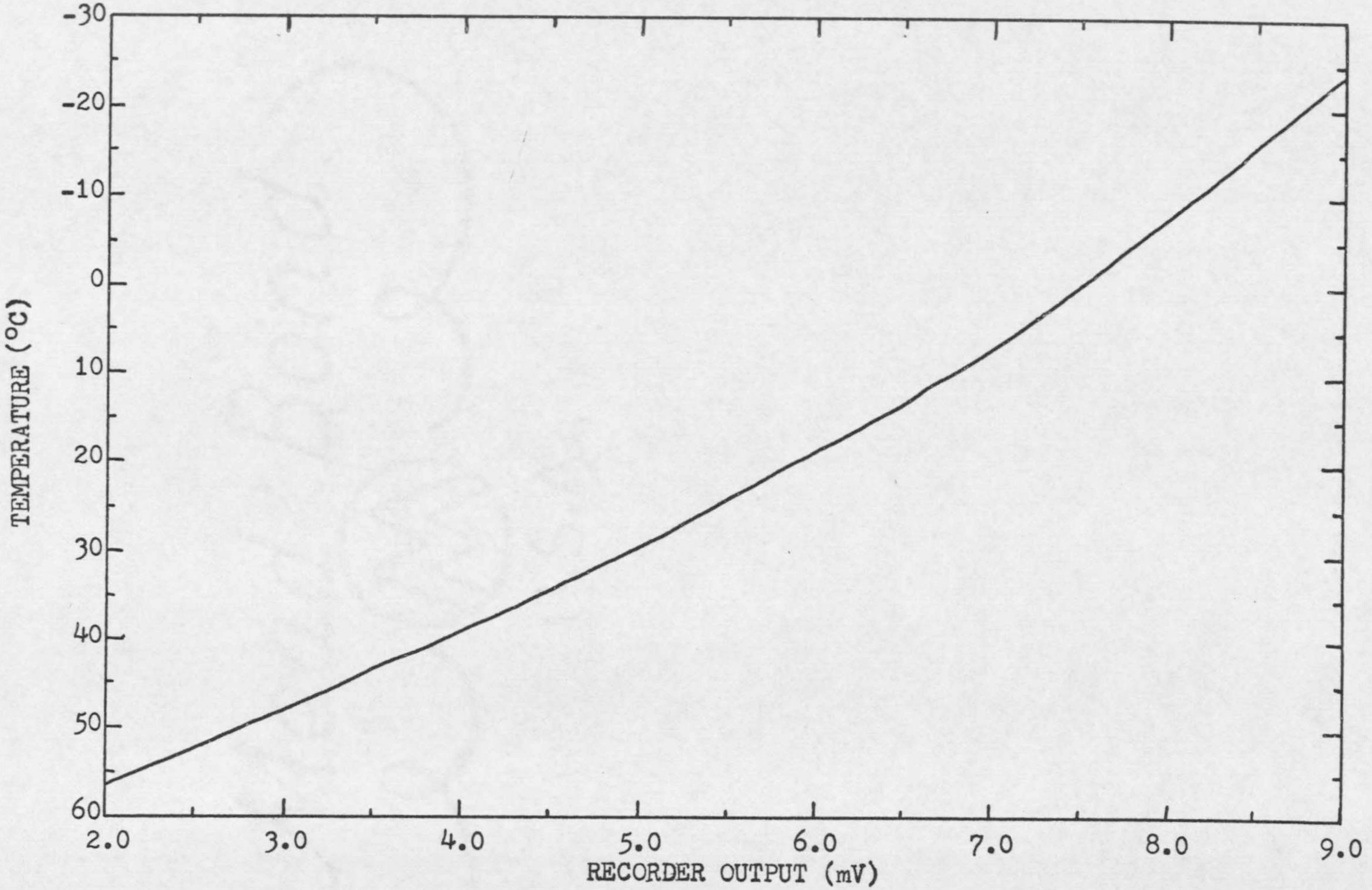

Figure 3.8 Calibration curve for the Barnes IT-3 infrared thermometer showing temperature versus millivolts output.

runs. The deviation of the individual curves obtained from each run about the mean curve is a measure of the accuracy of the instrument. The absolute accuracy was found to be ± 2.1C in the range below 0C and ± 0.3C in the range above 0C. These accuracy figures are calculated from the temperature represented by three standard deviations about the mean curve. For a normal distribution there is a 99.7 per cent probability that the true mean lies within three standard deviations of the sample mean. In the case at hand three standard deviations have been converted to temperature equivalents. This method assumes that no systematic error was present in the data and therefore all error contributions were random.

The results of the calibration revealed that the IRT does perform according to the temperature accuracy and resolution specifications claimed by the manufacturer. However, the instrument warm up time required to meet these specifications was one and one half hours as compared to the advertised period of one half hour.

Chapter 4

EMISSIVITY OF SNOW SURFACES

4.1 General Remarks

Investigating the emissivity of snow in its diverse crystalline forms presents a challenging problem from several aspects. The snow surface is not a sharply defined boundary such as is exhibited by a water surface. Rather, it is composed of ice crystals piled on top of one another with air pockets between the crystals. For the purposes of this paper the snow surface is defined as that layer whose vertical extent presents an effective radiating surface at infrared wavelengths. No attempt is made to ascertain the depth requirement necessary to fulfill this definition, although it is assumed to be less than a centimeter.

Crystalline shapes of freshly fallen snow range from plates and stellar crystals to columns, needles, irregular forms, and graupel, to name only a few. A good description of other forms often found in nature can be found in Magono and Lee (1968). Each type of crystal develops in a characteristic environment within a cloud. The hexagonal structure frequently associated with the term snow crystal does not always describe what is observed. Riming phenomenon may disguise the original crystal form and make it unrecognizable by the time it reaches the earth's surface. Collisions among snow crystals in falling may result in the formation of numerous nondescript ice fragments.

In addition to the variation in crystal form, the size distribution of the crystals and their orientation complicates the problem. Because a rough surface is a better emitter at infrared wavelengths than a smooth surface, an intuitive conclusion that a snow surface is a very good emitter might seem logical. The countless reflection surfaces of the crystal faces represent an essentially rough surface. The relative roughness of the surface may change with crystal size and orientation, however.

Snow metamorphism also contributes to variations in observed crystal types. Upon reaching the earth's surface, the crystalline structure of a snowflake is subjected to metamorphic influences. Temperature gradients and the action of wind are two of the most important of these influences. The metamorphic process tends to produce granular snow whose appearance takes the form of rounded ice grains rather than the original angular crystals. The metamorphosed granular snow may or may not possess the radiative properties of the parent snow crystals.

Another complexity which must be considered for emissivity determinations is the task of measuring the true surface temperature of the snow while leaving the surface unaltered. A review of Eqs. 2.10 and 2.11 reveals the importance of accurate surface temperature information for emissivity calculations. If temperature gradients are present in the first few millimeters, a unique temperature of the snow surface cannot be obtained by conventional means.

The conditions under which a program for calculating the emissivity of a snow surface are conducted may at times be adverse. The nature of the surface being investigated does not lend itself to laboratory analysis where environmental factors can be controlled. Instead, measurements must be made in the field in an environment which may be less than optimum. To this end the instrumentation must be such that elaborate preparations are not necessary for each measurement.

Desirable characteristics for an ideal observation site included an accessible location and one where snowfall was frequent and not contaminated by pollution particles from human activities. A power supply to run the instruments and a shelter to house them was also needed. Once a site was selected a method to determine the emissivity of the snow surface was required.

4.2 Design of the Measurement Technique

The method chosen to perform the emissivity tests was essentially that of Buettner and Kern (1965) with certain modifications of the procedure as proposed by Dana (1969). This approach involved the use of an apparatus called an "emissivity box" and the IT-3 radiometer. It was chosen for the following two reasons: the emissivity box was a device with the capability of field use, and its utilization required that only three infrared measurements be made for each emissivity computation. A desirable feature of this instrument was that it permitted an average surface temperature of the snow to be determined by radiometric means, thus eliminating the need for thermocouples or thermometers which provide only point values of temperature.

The emissivity box essential to the operation was acquired from the Department of Atmospheric Sciences, University of Washington, through the courtesy of Dr. K. Buettner and Dr. K. Katsaros. The development of the theory of the emissivity box presented below closely follows that of Dana (1969). A schematic diagram of the box is presented in Figure 4.1.

Basically, the box is a cylinder whose interior walls are surfaced with a thin film of gold to approximate a mirror surface with a very nearly perfect reflectivity in the infrared. The lid consists of a temperature controlled aluminum slab whose lower surface is grooved and painted with Parsons Black Optical Paint to approximate a blackbody. Two sliding lids with gold plated lower surfaces are attached in such a manner that they can be closed to cover the black top. The aluminum slab is maintained at a temperature different than that of the surface being investigated. For the majority of measurements made the temperature of the black top was maintained at 30C above the snow surface temperature. A 50C difference was maintained for only a few measurements made during the initial phase of the investigation. The sensing head of the IRT is seated on the aluminum lid looking downward at the surface through a small aperture. Readings are taken alternately with

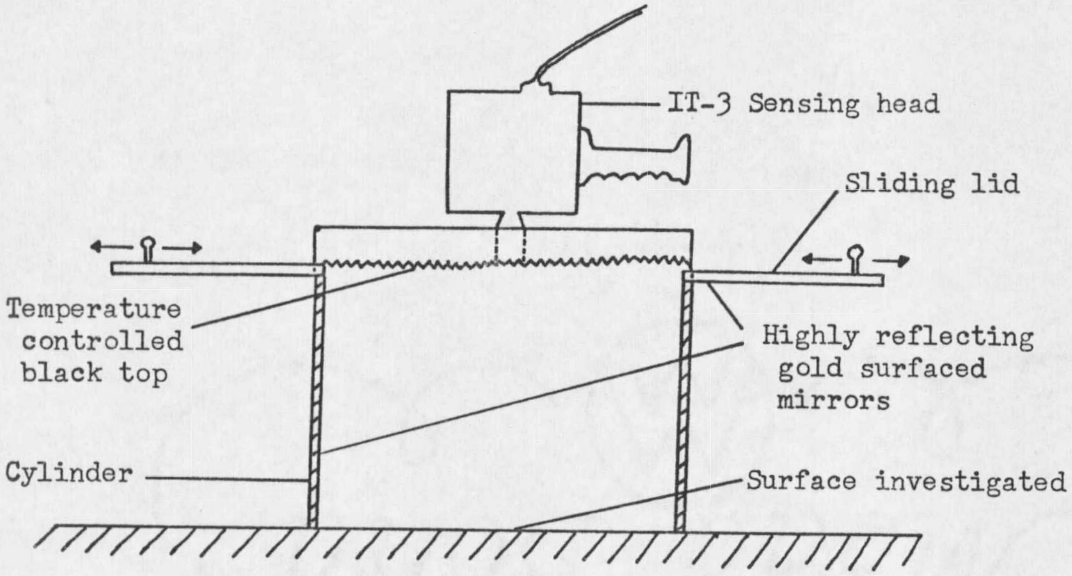

Figure 4.1 Diagram of the emissivity box and radiometer arrangement used to determine the emissivity of the surface forming the floor of the cylinder.

the highly reflecting lid in place and with the black lid in place. When the mirror lids are in place, the surface below is radiating very nearly as a blackbody. From the two measurements taken with the black and mirror lids in place, and a third measurement obtained by tipping the emissivity box on its side and looking at the black lid, the emissivity of the snow surface can be calculated. It should be borne in mind that the emissivity obtained in this manner is a spectral emissivity determined by the filter response of the radiometer.

The gold plated mirror surfaces are not perfect reflectors nor is the black top perfectly black at the infrared wavelengths utilized in the study. The reflectivity of the gold mirrors was determined by Buettner and Kern and by Dana to be between 0.98 and 0.99. They also state that the emissivity of the upper black lid is 0.985. From these figures it can be concluded that the assumptions of a black top and nearly perfect reflection at the mirror surfaces are not unwarranted.

The scientific basis for the emissivity box technique is based on the theory of radiation transfer between two infinite parallel planes formulated by Fleagle and Businger (1963). The infinite parallel planes are approximated by the highly reflecting sidewalls. In developing the equations which explain the radiative process occurring with the box the following notation will be adopted. The subscript f refers to the sample material forming the floor of the ϵ box and the subscript r refers to the roof of the ϵ box. The superscript m is used when the mirror lid is in place and b is used when the black lid is exposed. The effective blackbody radiance from the surface at temperature T_f is given by

$$B_f = \int_0^\infty q(\lambda)\ B(\lambda, T_f)\ d\lambda \tag{4.1}$$

Similarly, B_r denotes the value of the effective blackbody radiance of the lid.

The radiance N_f from the sample surface sensed by the IT-3 can be written

$$N_f = \epsilon_f B_f + (1 - \epsilon_f)\ N_r \tag{4.2}$$

where N_r is the radiance from the upper surface downward. It is possible to express N_r in terms of N_f as

$$N_r = \epsilon_r B_r + (1 - \epsilon_r)\ N_f \tag{4.3}$$

Eliminating N_r and solving for N_f gives

$$N_f = \epsilon_f B_f + (1 - \epsilon_f)\ (\epsilon_r B_r + (1 - \epsilon_r)\ N_f) \tag{4.4}$$

The radiance N_f^b when the black lid forms the top and the radiance N_f^m from the surface, sensed by the radiometer when the mirror lid forms the top, can be written in the form of Eq. 4.4. Then, subtracting N_f^m from N_f^b and solving for ϵ_f produces the equation

$$\epsilon_f = 1 - \frac{N_f^b - N_f^m}{(\epsilon_r^b B_r^b - \epsilon_r^m B_r^m) + (1 - \epsilon_r^b)N_f^b - (1 - \epsilon_r^m)N_f^m} \tag{4.5}$$

If it is assumed that $\epsilon_r^b = 1.00$ and $\epsilon_r^m = 0.00$, Eq. 4.5 becomes

$$\epsilon_f = 1 - \frac{N_f^b - N_f^m}{B_r^b - N_f^m} = \frac{B_r^b - N_f^b}{B_r^b - N_f^m} \tag{4.6}$$

It was previously noted that ϵ_r^b was not quite equal to 1.00 and ϵ_r^m was not identically zero. This results in Eq. 4.6 predicting a slightly higher value of ϵ_f than Eq. 4.5. The quantity B_r^b of Eq. 4.6 requires that the temperature of the black lid be known precisely. If the emissivity box is turned on its side and the black top viewed by the radiometer, the quantity N_f^b is obtained and can be substituted for B_r^b in Eq. 4.6 to yield

$$\epsilon_f = \frac{N_r^b - N_f^b}{N_r^b - N_f^m} \tag{4.7}$$

Dana has shown that after consideration of the emissivity box geometry and absorption by the walls and viewing cavity, Eq. 4.7 results in a surface emissivity value that need be corrected by only a small amount to arrive at the true emissivity. For surfaces with emissivities greater than 0.95 the correction is less than 0.002. The emissivity box used in this research is the same one for which Dana computed the corrections to be applied.

It should be noticed that all of the quantities on the right side of Eq. 4.7 are radiometrically obtained. Also, Eq. 4.7 does not require that the temperature of the snow surface be monitored.

All emissivity measurements for snow were carried out at a location fifteen miles northeast of Bozeman, Montana, in a mountain valley in the Bridger Range. The site was relatively free of contaminants related to human activity, was readily accessible, received frequent snowfalls, and was provided with a trailer house and electrical power. A plywood shelter was constructed as an annex to the trailer to serve as an unheated outdoor laboratory. All of the electronic instruments were housed within the heated trailer. The sensing head was also placed in the trailer when not in use to avoid temperature fluctuations in the internal reference cavity.

Snow samples were obtained by one of two methods. In the first method a thin sheet of masonite was slid under a layer of snow approximately six centimeters thick and removed, with care being taken not to disturb the surface. This technique was resorted to when the snow was crusted or when a snowfall had occurred the previous night. The second method was employed when snowfall was occurring. The sample boards were placed outside and snow was allowed to accumulate to a depth of several centimeters. The samples were then brought inside the shelter and stored until used. The storage period was generally less than an hour.

A calibration check of the IRT was made at two temperatures prior to each group of observations. A check at 0C was made by pointing the radiometer at a mixture of snow and water while it was stirred. Water was used because it has an emissivity in the spectral response region of the IT-3 of nearly unity as evidenced by data in Table 2.1. Snow was utilized as a convenient means of establishing a temperature of 0C. A second reading was obtained by viewing the blackbody cavity of Figure 3.5 whose temperature, measured by thermocouples, was that of the ambient air in the shelter.

All emissivity values for a particular snow surface type were obtained by averaging from six to fifteen sample cases. Replication of the crystals for each snow type was done and is reported in section 4.4.

The emissivity box was adjustable to several different cylinder heights. A 15 centimeter high cylinder adjustment was used to allow for clearance between the snow surface and the lid. After each sample the interior of the cylinder was thoroughly cleaned of any water film which might initiate a change in the reflectivity of the sidewalls. To accomplish this the walls were wiped first with a soft, dry cloth to remove excess water drops and then with a cloth dampened with alcohol to remove any remaining moisture.

A minor modification of the lower base of the cylinder was undertaken to eliminate the direct reflection component from the radiometer sensing head back into the sensing head when viewing the snow surface. This was achieved by introducing a slight bevel to the base of the cylinder, preventing it from sitting in a level position.

Figure 4.2 is a photograph of the snow boards and the area where the snow samples were collected. Figure 4.3 is a photograph of the arrangement of the emissivity box, radiometer, and snow sample in preparation for a set of measurements.

4.3 Discussion of Errors

The errors inherent in the emissivity box technique have been discussed in detail by Kern (1965) and Dana (1969). Their error analysis reveals that systematic errors in determining the radiance values necessary for the computations lead to emissivity errors less than 0.1 per cent. The most important source of error is determining the equivalent blackbody temperature of the snow surface when the black lid and the mirror lid constitute the upper surface. If the temperature error when the mirror lid is in place is of the same magnitude and in the same direction as the error when the black lid is in place, the error in the emissivity value is small. These errors might be expected to be in the same direction when one considers that the IT-3 yields more accurate relative temperature measurements than absolute measurements. If, however, the snow surface is warmed by radiative heating when the black top is in place compared to when the mirror lid

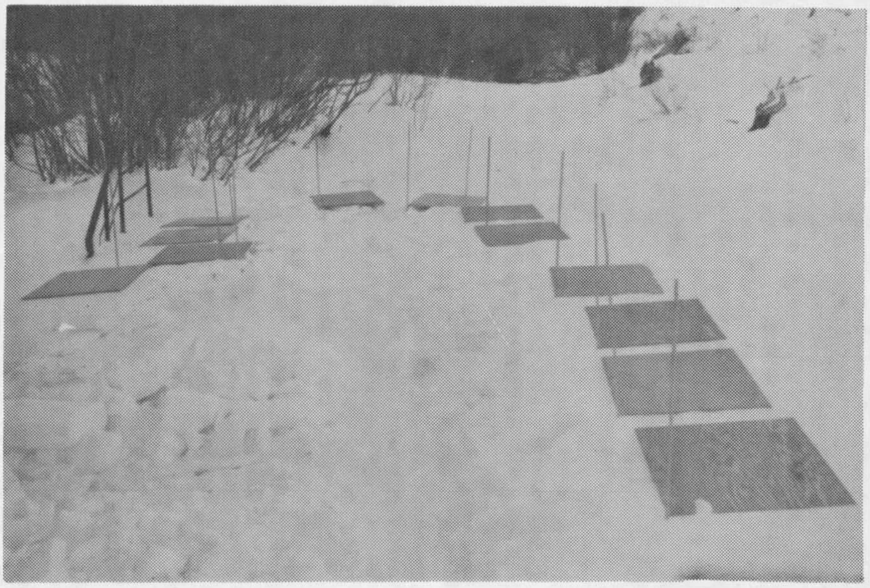

Figure 4.2 Photograph of the snow boards and the area where the snow samples were collected.

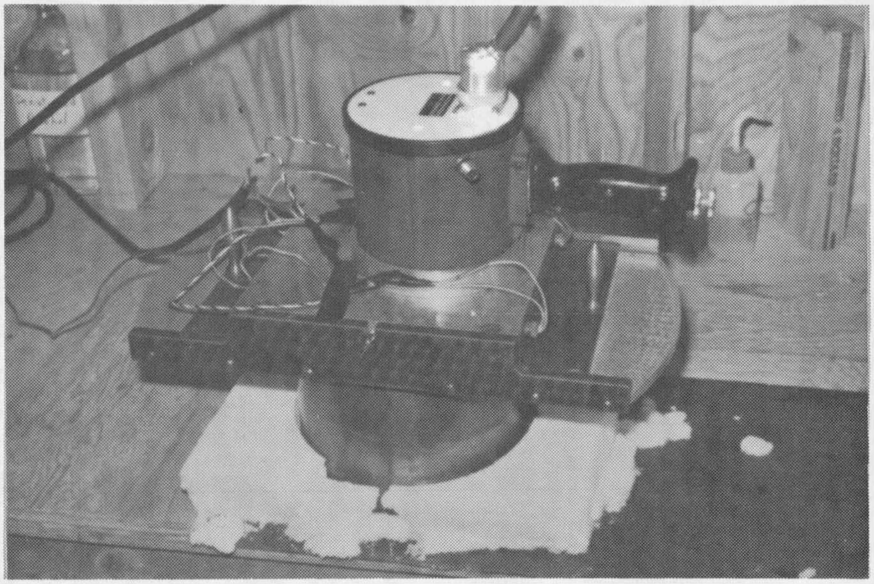

Figure 4.3 Photograph of the arrangement of the emissivity box, radiometer, and snow sample in preparation for a set of measurements.

is in place a serious error would result in the derived emissivity value. Table 4.1 indicates the magnitude of the error which this situation would initiate. The error is computed by assuming a true emissivity value of 0.989 and a true snow surface temperature of -10.0C, as determined by the IT-3 with the mirror lid in place. The temperature of the black lid is assumed to be 20C.

Table 4.1 Induced error in emissivity caused by radiative heating of the snow surface with the black lid in place.

Temperature rise due to radiative heating (°C)	Computed Emissivity	Per cent Error
0.0	0.989	0.00
0.5	0.982	-0.70
1.0	0.966	-2.33
1.5	0.955	-3.44
2.0	0.943	-4.66
2.5	0.928	-6.18
3.0	0.915	-7.50

From Table 4.1 it can be seen that the net effect of a rise in snow surface temperature with the black lid exposed is a reduction in the computed emissivity value.

To test the hypothesis that radiative heating was a problem, a copper-constantan thermocouple, of 0.25mm diameter, was placed on the snow sample surface and carefully covered with a very thin layer of snow crystals. The temperature of the black lid was maintained at a temperature 30C warmer than the snow surface. The temperature of the snow surface was monitored with the thermocouple for ten-second intervals with the mirror lid and the black lid alternately forming the top of the emissivity box. Shorter time intervals on the order of several seconds would have been desirable but since the thermocouple was monitored manually with a potentiometer, this was not practical. On the average no heating effects were observed when the mirror lid was in place, as would be expected since gold possesses a very low emissivity. When the black lid was exposed for ten seconds an average rise of 2.52C was observed.

The same procedure was done using the IT-3 to monitor the snow surface temperature. Once again no rise in temperature was observed with the mirror lid in place, but an average rise of 2.24C was observed with the black lid exposed.

Using a temperature rise of 2.5C and Table 4.1 yields an apparent error of -6.18 per cent. This would indicate that under the conditions used to develop Table 4.1 the computed emissivity would be 0.928. The value 0.928 assumes that the value of N_f^b is calculated from the snow surface temperature obtained with the IRT after ten seconds with the black lid exposed.

To minimize the effect of radiative heating and yet allow the recorder to fully respond to a change in signal when the mirror lid is opened to reveal the black lid, a five second exposure time for the black lid was chosen. In practice the temperature used to calculate

N_f^b was obtained 3.6 seconds after the mirror lid was opened, corresponding to the third data point printed by the recorder after the black lid was exposed. This procedure produced results which are believed to be relatively free from the effects of radiative heating. In support of this, a series of emissivity measurements for the same snow surface were made varying the temperature of the black lid. Table 4.2 is a summary of the results of these measurements.

Table 4.2 The effect of temperature variation on the calculated emissivity of a snow surface at -3.0C.

Temperature of black lid (°C)	Emissivity	Number of observations	Standard deviation
20	0.980	10	0.011
30	0.978	13	0.007
50	0.976	10	0.004

These results reveal a minor trend toward lower emissivities for increased lid temperatures.

To insure that the emissivity box and radiometer were yielding surface emissivity values which were comparable with published values for surfaces other than snow, a series of emissivity measurements were made for water, plywood, formica, and aluminum foil. The average spectral emissivity for each material is given in Table 4.3 along with the value published by Kern (1965), who used an emissivity box of different design. Both emissivity values are for the spectral interval from 8 to 14 microns. Additional emissivity data for these surfaces for the same spectral interval were not found in the literature. From Table 4.3 it may be seen that the emissivity values are in reasonably close agreement considering that the actual test surfaces were not the same in both cases. The only exception is aluminum foil. Its higher emissivity may have been due to the presence of an oxidation layer on the surface since it was not cleaned before the measurements were taken.

Table 4.3 Comparison of spectral emissivities for similar surfaces in the 8 to 14 micron region.

Surface	Measured Emissivity	Number of Samples	Emissivity (Kern, 1965)	Number of Samples
Water	0.993	8	0.994	12
Plywood	0.949	6	0.962	10
Formica	0.947	6	0.937	16
Aluminum Foil	0.070*	6	0.010	15

*Dull side of foil, with possible oxidation layer on the surface.

In conclusion it can be stated that the emissivities of snow surfaces obtained by the emissivity box technique are reliable. When the influence of radiative heating is analyzed it is seen that the net effect is to produce an emissivity lower than the actual value. Thus, the actual emissivity values are at least as high as the calculated emissivity figures.

4.4 Replication of Snow Crystals

For each set of emissivity measurements replicas of the crystal form were preserved according to a technique developed by Schaefer (1949). The technique consists of capturing the structure of snowflakes in a dilute plastic solution which does not dissolve ice. The mixture is a one per cent solution of polyvinyl formal dissolved in ethylene dichloride. Polyvinyl formal can be obtained under the trade name Formvar 15-95.

The method used for this research was to apply a coat of formvar to a two-inch square glass slide after both had been cooled below OC. The slide was then exposed to catch the falling flakes for a period of thirty seconds to one minute. Upon falling into the plastic solution the flakes become coated with a thin film of the solution. The solvent evaporates and the ice sublimates through the plastic film leaving an impression of the crystal. The slide is placed in an environment colder than OC and allowed to cure for a period of twelve to twenty-four hours, or until no trace of the solvent remains. In the manner described, a permanent record can be obtained of the crystalline form of falling snowflakes. Schaefer (1949) reported that an alteration in the strength of the formvar solution from one per cent to five per cent permits replicas to be made of crystals forming a snow surface. Replications of crystals from the snow surface may then be compared with replications of falling snow crystals. To replicate crystals off a snow surface a cooled slide is coated with the five per cent solution of formvar, pressed firmly against the snow surface, and allowed to cure in the same manner as described.

Both one per cent and five per cent solutions were utilized to obtain replicas of the snow crystals for this investigation. It was discovered that the replicas obtained from the snow surface using the five per cent solution were not of as high a quality as the replicas obtained from falling flakes. In addition, it was not possible to adequately replicate clusters of snowflakes larger than a few millimeters in diameter with the method used. Such flakes were a common occurrence in the study area, and usually consisted of dendrite or stellar crystals interlocked to form a single giant flake. The crystals as observed through a ten power hand lens were frequently rimed.

The effects of wind on newly fallen snow tended to result in a crusted snow surface composed of ice crystal fragments. Ice crystals on the crusted snow surface were smaller than most falling crystals observed. They were difficult to identify in terms of their original structure. The crusted snow surface appeared to the unaided eye to be smoother than the snow surface existing subsequent to a new snowfall. This appearance was deceptive, for upon closer examination the smoother appearance was attributed to the existence of larger numbers of small ice forms comprising the surface layer. The total effect was to increase the exposed surface per unit area.

The range of snow crystal types for which emissivity measurements and replications were made was not large. The spectrum of crystal types studied was confined to newly fallen graupel, dendrites, and stellar crystals, as well as snow crusted by wind and melt phenomenon. Possible changes in the emissivity of a snow surface cause by equi-temperature metamorphism over extended periods were not investigated because the opportunity did not present itself during the study period due to the high frequency of snowfalls at the study site.

4.5 Results of Emissivity Investigations

Spectral emissivities of snow surfaces studied in the range of temperatures encountered during the observation period were found to be quite high. Table 4.4 summarizes the results of the emissivity measurements. The emissivity values listed in the table are averages of from six to 15 samples. In addition, the temperatures given are average temperatures of the snow surfaces taken with the IRT during the time each series of measurements were made. Actual temperatures of the snow surfaces ranged from -1 to -18C at various times during the study. A number of interesting points are apparent from the data of Table 4.4.

All emissivities are higher than 0.96 indicating that snow is an approximate blackbody radiator for the range of conditions investigated. Also, the range of emissivity values is relatively small for the snow surfaces (0.966 to 0.989). A dependence of the total emissivity of a snow surface on its temperature reported by Dunkle _et al_. (1955) is not

Table 4.4 Average emissivities for various snow surfaces and crystal types.

Case Number	Number of Samples	Average Emissivity	Standard Deviation	Snow Surface Temperature (°C)	Crystal Type	Description
1	7	0.984	0.003	- 4	Clumps of dendrites and stellar crystals	Crusted snow.
2	8	0.973	0.012	-11	Clumps of dendrites and stellar crystals	Snowfall previous night, not crusted.
3	10	0.982	0.004	- 5	Fragmented crystals	Wind crusted snow.
4	8	0.976	0.005	- 9	Fragmented crystals	Snowfall previous night, crusted by wind.
5	6	0.966	0.006	- 9	Clumps of dendrites and stellar crystals	Freshly fallen snow.
6	11	0.989	0.004	-11	Fragmented crystals	Wind crusted snow.
7	8	0.977	0.011	- 8	Clumps of dendrites and stellar crystals	Snowfall previous night, not crusted.
8	10	0.976	0.009	- 3	Clumps of dendrites and stellar crystals	Freshly fallen snow.
9	10	0.980	0.011	- 3	Rimed stellar crystals	Freshly fallen snow.
10	10	0.976	0.004	- 3	Rimed stellar crystals	Freshly fallen snow.
11	13	0.978	0.007	- 3	Irregular forms and stellar crystals	Freshly fallen snow.
12	15	0.989	0.009	- 7	Refrozen crystals	Crusted snow from melt and refreezing.
13	15	0.976	0.010	- 4	Graupel on stellar crystals	Freshly fallen snow.
14	15	0.971	0.007	- 2	Stellar crystals	Freshly fallen snow.
15	14	0.974	0.006	-11	Stellar crystals	Snowfall previous day, not crusted.
16	10	0.988	0.005	-10	Refrozen crystals	Crusted snow from melt and refreezing.
17	15	0.976	0.007	- 4	Rimed stellar crystals and graupel	Snowfall previous night, not crusted.

shown, although it should be noted that Dunkle's data are not strictly comparable. Changes in crystal type appear to have a minor effect on emissivity with one exception. Crusted snow exhibits a slightly higher average emissivity compared to newly fallen snow. The average emissivity for crusted snow is 0.985 (6 cases) and for freshly fallen snow it is 0.975 (11 cases). The difference is quite small, 0.010, yet a plausible explanation can be offered for its existence.

Two mechanisms are primarily responsible for the crusting of a snow surface: 1) warming and refreezing; and 2) the action of wind. There is a tendency in both processes to result in the production of more ice forms per unit area. In the first process warming and refreezing causes the weaker appendages on crystals to break off. This is particularly true of stellar and dendritic crystal types. Wind action also produces more ice particles per unit area by causing ice crystals to collide and break up. Ice crystal fragments formed by both processes have the net effect of presenting a surface which is rougher than the original surface in the sense that increased surface area is exposed. Just as adding grooves to the black lid of the emissivity box increased the surface area and consequently its blackness, so too increasing the surface area of a layer of snow increases its blackness. Another factor may be responsible for the slight emissivity differences observed. Since crusted snow has a density higher than newly fallen snow, it may also be possible that in some unexplained manner density affects emissivity.

When all the emissivities of Table 4.4 are averaged, a mean emissivity for all snow surfaces examined is found to be 0.978. This is much higher than the range of values from 0.43 to 0.66 calculated from data reported by Miller (1963) for a similar spectral interval. It is not possible to compare this mean emissivity with the total emissivities given by other authors because of its limited spectral validity. But, it is possible to say with a high degree of assuredness that the mean emissivity calculated is an accurate and realistic figure for the 8 to 14 micron region of the spectrum. Further, it can be stated that variations about this mean value are small.

In addition to the emissivity measurements made for snow surfaces, tests were conducted to determine the emissivity of solid ice and of hoar frost crystals, both grown in a chest type freezer. Hoar frost crystals were grown in an attempt to duplicate the situation of a snow surface covered with surface hoar. A solid ice sheet 0.4 centimeters thick was examined in an effort to determine the emissivity for the case when a solid ice crust forms on a snowpack. The hoar crystals were grown at a temperature of -9.5C. Their crystalline structure closely resembled the cup-like shape of depth hoar crystals. Their size varied from 8 to 0.5mm in the largest dimension. The average emissivity of the hoar crystals calculated for four samples at a temperature of -9.5C was 0.979, and the standard deviation was 0.004.

Four samples of solid ice, also at a temperature of -9.5C, yielded a mean emissivity of 0.983 with a standard deviation of 0.007. The mean emissivity for the hoar crystals is close to typical values of newly fallen snow, while the average emissivity for ice is comparable to the mean emissivity of crusted snow. Similarity in the high emissivity of solid ice and crusted snow leads one to suspect a dependence of emissivity on density as well as crystal numbers. No conclusive statement to this effect may be made, however, due to the limited number of cases for solid ice coupled with the possible measurement errors inherent in the method.

Chapter 5

THE EFFECT OF REFLECTED RADIATION AND ATMOSPHERIC ABSORPTION

5.1 General Remarks

Radiometers which sense thermal radiation have an inherent shortcoming in that they are unable to discern the difference between the radiance of a surface due to its temperature and the radiant energy reflected by the surface. The radiance which is received at the sensing element is thus the sum of the intrinsic radiant energy of the surface being viewed and the reflected component from other sources of thermal energy. Primary sources of reflected radiation are the sky and nearby objects. Sky radiance is composed of four components: 1) radiation from extra-terrestrial sources; 2) radiation from excited atoms and molecules in the upper atmosphere; 3) scattered solar radiation; and 4) thermal emissions by atmospheric constituents. The first two components of sky radiance are so small as to be completely negligible, while the third is important only at short wavelengths. Atmospheric emission, however, cannot be neglected, since the energy available from this source is almost wholly in the infrared region.

Because the reflectivity of most natural surfaces is small in the 8 to 14 micron spectral band (from one to six per cent, except for certain minerals), reflected radiation is not a serious problem for most radiometric surface temperature determinations. The variability in surface temperature from one point to another, resulting from micro-scale considerations, often exceeds any variability which would be encountered due to reflected radiation. Nevertheless, it is important to understand the manner in which reflected radiation affects surface temperature measurements, and the magnitude of the influence which may be expected.

Investigation of the effect of reflected radiation on snow surface temperature measurements was not emphasized in the research. Only a cursory look at the effect of reflected radiation was pursued because of the high average emissivity of snow (and correspondingly, low reflectivity) and reduced accuracy of the IT-3 at the low temperatures encountered. A brief treatment of reflected radiation is presented so that the reader may gain an understanding of the influences which may be expected for various meteorological conditions.

5.2 The Effect of a Clear Sky

The radiation which a radiometer senses when looking vertically downward on a surface is composed of blackbody radiation from the surface and reflected radiation from the sky and surrounding objects. Snow, like most natural surfaces, is a diffuse reflector of infrared radiation. Therefore, the hemispherical radiance of the entire sky contributes to the reflected energy. If the radiation from nearby objects is neglected, the radiance N_s incident on the detector from the surface at temperature T_s can be written in the form

$$N_s = \int_0^\infty \epsilon_s q(\lambda)B(\lambda,T_s)\, d\lambda + \int_0^\infty (1 - \epsilon_s)q(\lambda)G(\lambda,T_a)\pi^{-1}\, d\lambda \qquad (5.1)$$

where T_a = average blackbody temperature of the sky

$G(\lambda,T_a)$ = sky radiant emittance

and other terms are as defined previously. The second term on the right of Eq. 5.1 represents the radiance of the sky reflected diffusely by the surface. It can be seen that the net effect of reflected sky radiation is to increase the radiance, and thus the indicated radiant temperature of the surface, in an amount proportional to the mean spectral reflectivity of the surface and the mean radiant temperature of the sky. This approach greatly simplifies the actual situation.

Strictly speaking, the radiance from the sky cannot be characterized as originating from a hemispherical shell at a constant temperature. Rather, it is a complex condition in which the atmospheric constituents are radiating at different temperatures at varying heights in the atmosphere. The effective blackbody temperature of the atmosphere is found to vary markedly with changing elevation angle. Figure 5.1 demonstrates this phenomenon. In the figure, spectral sky radiance of a clear sky is substituted for blackbody temperature. Spectral radiance of the sky in the 8 to 14 micron region is shown to decrease with increasing elevation angle. This is attributed primarily to the decrease in path length with increasing elevation angle. Figure 5.1 depicts the situation for a relatively cold, dry atmosphere. With

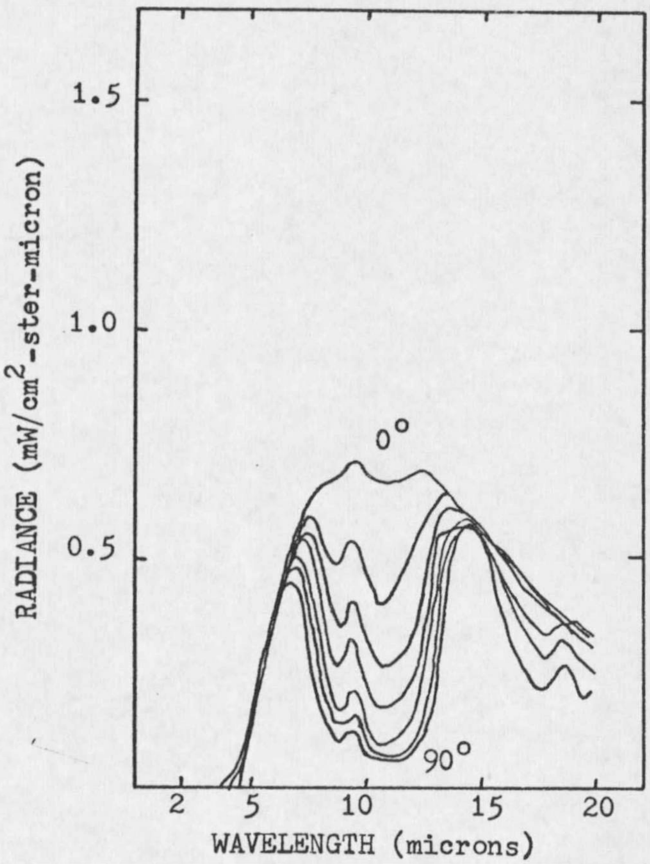

Figure 5.1 Spectral radiance of a clear sky for elevation angles of 0°, 1.8°, 3.6°, 7.2°, 14.5°, 30°, and 90°. The decrease in radiance with increased elevation angle illustrates the change in the radiant temperature of the sky with changing elevation angle. Spectra are for Elk Park station, Colorado, 11,000 feet above sea level, when the ambient air temperature was 8C. (after Bell et al., 1960)

increased atmospheric temperature and additional water vapor the spectral radiance would be substantially increased at all wavelengths. The reflected component from a surface under clear sky conditions is variable and not readily estimated. It is known that for low ambient temperatures and low atmospheric water vapor content the contribution of reflected sky radiance under a clear sky will be less than for a cloud covered sky. It will also be small in comparison to the blackbody radiance from the surface determined by its temperature and emissivity.

Lorenz (1966) has calculated the difference between the true surface temperature and the radiation temperature obtained with a radiometer similar to the IT-3 to be slightly greater than 1C for clear sky conditions. This calculation was obtained using actual spectral radiance values for a clear sky with an ambient temperature of -3C, a postulated diffuse surface with an emissivity of 0.975, and a surface temperature of -10C. The 1C difference between actual and radiant temperature indicated by his calculation is the total difference produced by an emissivity less than unity and the reflected radiance of a clear sky. This is very nearly the temperature difference which would be expected for a surface with an emissivity of 0.975 if no reflected radiation was present as evidenced by examination of Figure 1.3. Thus, it may be concluded that the reflected radiance of a clear sky can be expected to contribute an equivalent temperature difference of only a few tenths of a degree Celsius for conditions normally encountered over snow surfaces. It should be noted once again that the effect of reflected radiation is to bring the radiant temperature of a surface into closer correspondence with the actual surface temperature, slightly counteracting the effect of an emissivity less than unity. Griggs (1968) has calculated the effect of reflected radiation from a clear sky for a diffuse surface with an emissivity of 0.99. The effect is to give a temperature difference of 0.13C, which compares favorably with the results of Lorenz.

From the above considerations it appears that reflected radiation from a clear sky increases the radiant temperature of a snow surface with an emissivity of 0.978 by one to three tenths of a degree Celsius above that which would be recorded in the absence of reflected radiation.

5.2 The Effect of a Cloud-Covered Sky

When the sky is either partially or wholly covered with clouds, it presents a radiation source with a much higher radiant temperature than the clear sky. The radiant temperature of a cloud-covered sky is a function of cloud type, height, amount of cloud cover, and temperature, and can change rapidly in a short period of time. Figure 5.2 illustrates some observations of changes in the effective blackbody temperature of the sky, which ranged from completely clear to overcast conditions. When the sky was clear the temperature was below the capability of the IRT and was not recorded. Progressive warming was

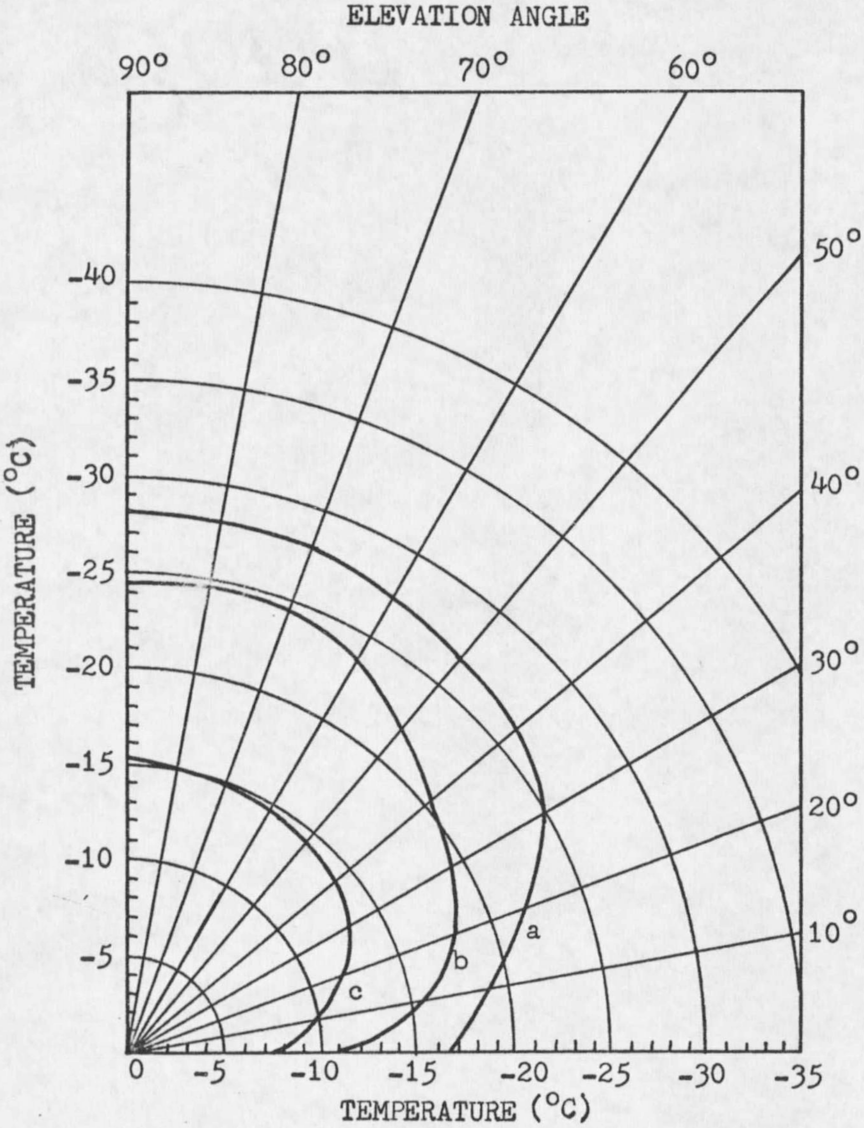

Figure 5.2 Plot of radiant sky temperature versus elevation on Feb. 2, 1971, at Bozeman, Montana, elevation 5,000 feet above sea level. Curve a, 1337 MST, FAA estimated cloud base 18,500 ft. broken, 29,500 ft. broken; curve b, 1501 MST, estimated 18,500 ft. broken, 29,500 ft. overcast; curve c, 1622 MST, estimated 14,500 ft. broken, 22,500 ft. overcast, snow showers observed.

apparent as time passed, until a cloud base temperature of -15.2C was observed directly overhead when the sky was completely overcast. This temperature can be considered to be very nearly the actual cloud base temperature because water is highly emissive in the infrared and closely approximates a blackbody under overcast conditions (Bell, et al., 1960).

Griggs (1968) computed an average radiant temperature increase of only 0.4C on an ocean surface due to reflected radiation from an overcast sky composed of low-lying stratus clouds. Further information on prevailing meteorological conditions was not given. Meteorological conditions at sea level over an ocean surface are significantly different than over a mountain snowpack in winter. For this reason an oversimplified example of the temperature influence which might be expected from reflected sky radiation off a snowfield was calculated. The following conditions were postulated for the example: a snow surface with an emissivity of 0.98 and an actual snow surface temperature of -5C under a low overcast sky whose cloud base was at -10C. Neglecting any absorption effects and assuming that the cloud cover radiates as a blackbody, an expected temperature difference of 0.6C was computed due to reflected radiation. The 0.6C value is the temperature increase which would be detected by a sensitive radiometer when compared to the radiant temperature of the snow surface with no reflection component. More accurate estimates of equivalent temperature increases due to reflection from cloudy or partially cloudy skies cannot be given because of the highly variable character of cloud cover and surface conditions.

5.4 The Effect of Nearby Objects and Atmospheric Attenuation

It is difficult to assess the contribution to the reflected radiation sensed by a radiometer from surrounding sources other than the sky. Both spatial and geometrical relationships, in addition to temperature differences, must enter into the analysis. The problem has not been investigated in detail, primarily because with the system used it can be generally be neglected without affecting the accuracy of the measurements. The validity of this approach is borne out when one considers that the reflection component emanating from nearby objects usually originates only from low elevation angles with respect to a horizontal surface and results in a minimal reflected contribution.

Atmospheric attenuation in the column of air between the target and observer may constitute an added consideration in certain instances. Modification of the radiation from the time it leaves the surface until it is detected at the radiometer is a result of atmospheric absorption and emission, principally by water vapor and carbon dioxide. Employing a radiometer which "looks" through the infrared window between 8 and 14 microns and restricting observation to short optical path lengths minimizes this absorption effect. Lenschow and Dutton (1964) reported that corrections for atmospheric absorptivity during aerial observations below altitudes of 300 meters were negligible. Lorenz (1966) reduces this distance to 100 meters. Corrections for longer viewing distances can be determined by several methods (eg. Griggs, 1968). The problem is further considered in the airborne portion of this study reported in the following chapter.

Chapter 6

AIRBORNE TEMPERATURE MEASUREMENTS OVER SNOWFIELDS

6.1 General Remarks

Since the work of Lenschow and Dutton (1964), numerous investigations including Fujita, et al. (1968) and Holmes (1969), have utilized airborne radiometers for surface temperature measurements. Addition of an aircraft-mounted temperature sensor provides the capability for monitoring the temperature structure in three dimensions. The mobility of an airborne system is its major advantage. Its value is obvious for instances where temperature information is desired in remote and relatively inaccessible environments. Large areas may be covered in short periods of time to provide an accurate portrayal of the temperature regime of the surface and overlying lower atmosphere.

After it was resolved that snow has a very high emissivity in the spectral range of the IT-3, several airborne case studies were conducted. The purpose of these studies was to determine the operational feasibility of using the IT-3 in an airborne mode to detect and map snow surface temperature gradients in mountainous terrain. Also, comparisons between snow surface temperatures determined by the IT-3 and shelter level temperatures were to be made.

All aerial measurements were conducted from a twin engine Piper Apache aircraft. The sensing head of the IT-3 was pointed downward through a hole in the floor. Power for the IRT and recorder was provided by a d.c. to a.c. converter connected to the electrical system of the plane. Air temperature at flight altitude was measured by either a thermometer mounted on the windshield of the plane or a thermistor mounted in a vortex tube attached to the underside of the plane. These sensors were found to agree with one another to within 0.5C.

6.2 Results of Aerial Measurements

On January 12, 1971, aerial observations of snow surface temperature were made in the Gallatin Valley near Bozeman, Montana. The flight line extended from the Horseshoe Hills in the north to the Spanish Breaks in the south, and followed a topographical profile of the valley. Snow surface radiant temperatures recorded on the flight are presented in Figure 6.1. Altitude above the snow surface was approximately 200 feet and ground speed averaged 120 mph. The valley was blanketed with 10 to 12 inches of snow which had fallen within the previous 24 hours. An intense temperature inversion was present in the valley which was under the influence of an arctic air mass. Cloud cover estimated by FAA personnel at the Bozeman Airport consisted of scattered clouds at an elevation of 9,500 feet above mean sea level (msl) and overcast conditions at an elevation of 14,500 feet msl. Wind conditions at the surface were calm. Radiant temperature of the snow surface depicted in the graph is an average obtained from the recorder trace. Actual fluctuations were on the order of one to two

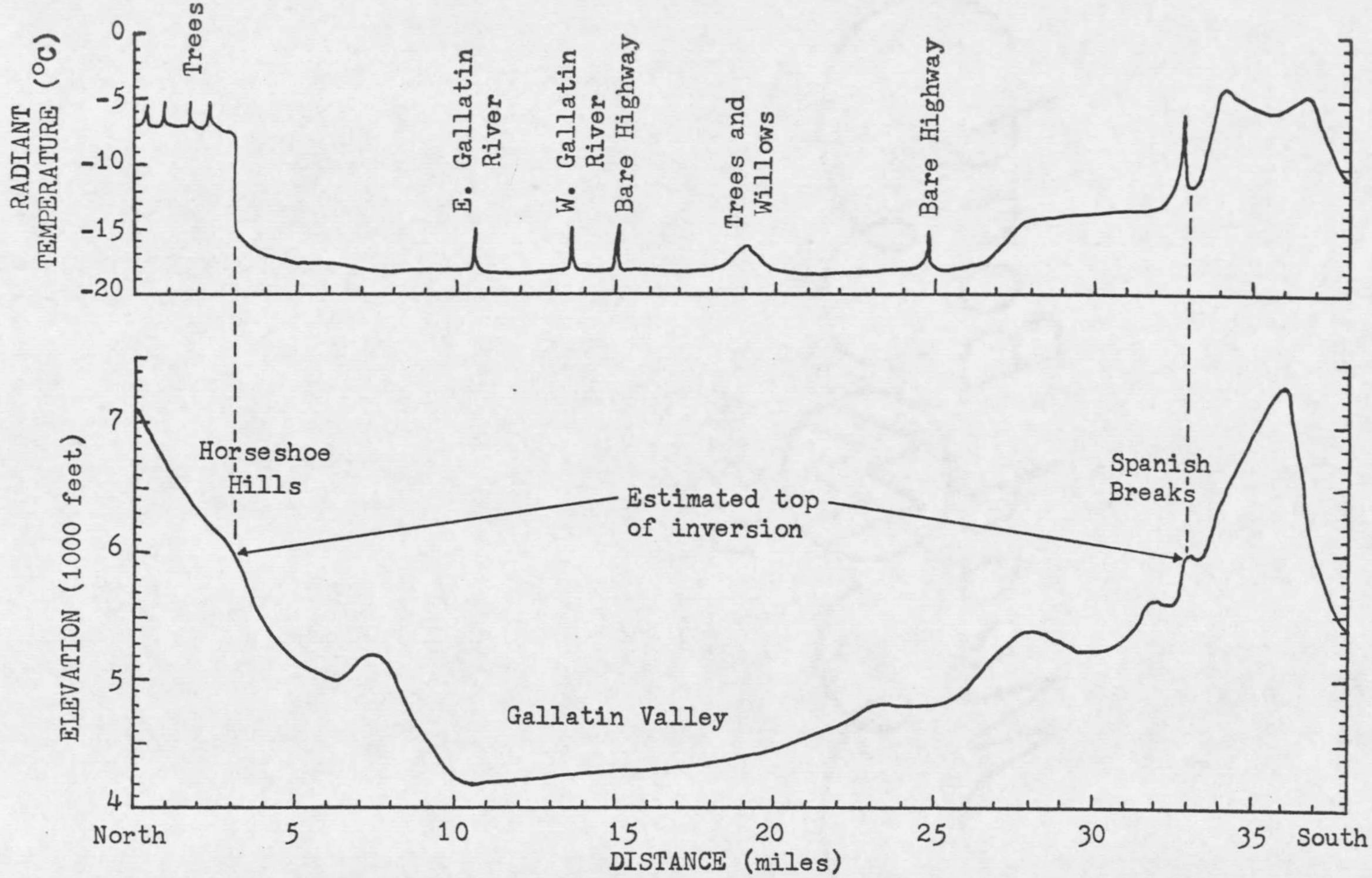

Figure 6.1 Plot of the radiant snow surface temperature obtained with an airborne IT-3 radiometer for a cross sectional profile of the Gallatin Valley, Montana. The flight was conducted on January 12, 1971, at 1445 MST during a strong temperature inversion in the valley.

degrees Celsius.

Figure 6.1 illustrates graphically the estimated level of the top of the temperature inversion located by mapping the surface temperature profile along the topographic profile. At the intersection of the inversion top and the surface a sharp temperature change was noted. In this manner the inversion top was estimated to be at about 6,000 feet msl. This determination is in good agreement with the inversion top estimated from examination of the vertical profile shown on Figure 6.2. The profile was constructed using aircraft temperature observations, temperatures recorded by thermographs in the Gallatin Valley and on the slopes of the Bridger Mountain Range forming the east edge of the valley, and FAA shelter level temperature measurements at the Bozeman Airport.

The radiant temperature averaged -18.5C on the valley floor. This corresponded closely with the ambient air temperature of -21C observed 1.5 meters above the surface at the airport some six and one half miles from the flight path, and -18C recorded by a thermograph in a weather shelter, also on the valley floor about ten miles from the flight path. The relatively warmer temperature of the highways and trees is due to radiant heating of surfaces not covered by snow. Figure 6.1 demonstrates the ability of an airborne radiometer to accurately detect temperature gradients on snow surfaces and to locate air mass boundaries at their intersection with the surface.

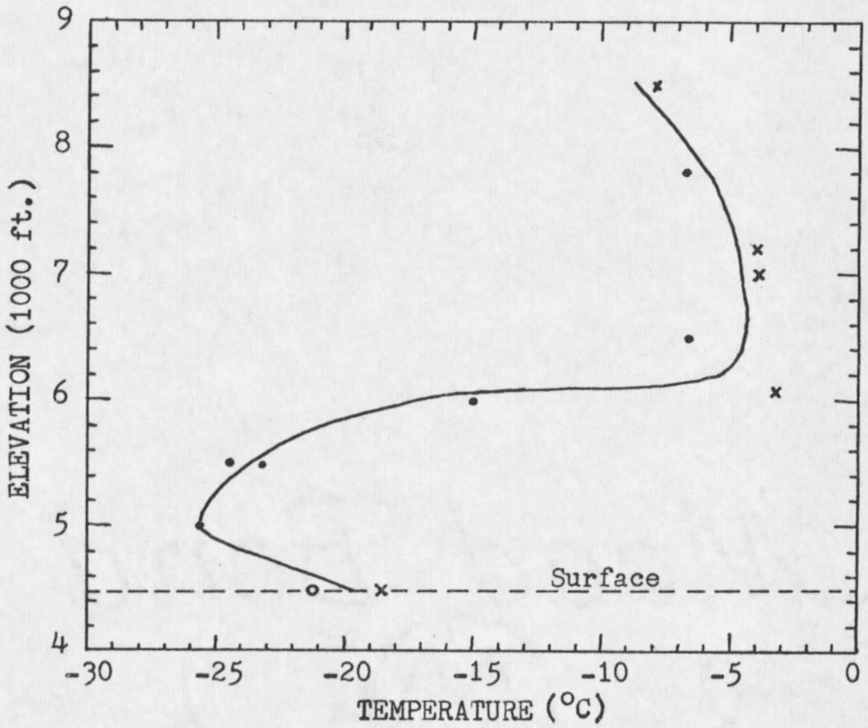

• Aircraft observation
x Thermograph observation
o FAA observation

Figure 6.2 Reconstruction of the vertical air temperature profile existing above the Gallatin Valley during the aerial observations of January 12, 1971. A prominent inversion whose top is at approximately 6,000 feet is the dominant feature.

Another case study was conducted on March 6, 1971, in the Centennial Valley of extreme southwestern Montana. Again the valley was under the influence of an arctic air mass and an inversion was present. However, this mountain valley was covered with snow from one to four feet in depth. The valley floor elevation is 6,600 feet msl. Clear skies prevailed throughout the measuring period. The radiometric surface temperature was monitored from approximately 100 feet above the surface at an average ground speed of 150 mph. The flight path was from northwest to southeast. Results of the flight are given in Figure 6.3.

Radiant temperature of the surface is again an average temperature along the flight path. The inset shows the actual variation in the temperature trace for a selected portion of the record. Relatively high temperatures recorded on the northwest slopes are due to exposed south-facing rock ledges heated by solar radiation. The cold surface of the valley bottom (-16C) may be due to prior radiational cooling and resultant cold air drainage from the surrounding slopes. On the south slopes of the valley over an almost level area a three to five degree Celsius temperature rise was noted. This might be explained by the fact that this area intercepts more solar radiation per unit area than either the slope above or below it, since both face away from the sun. Actual temperatures at the snow surface were not available for comparison purposes because of the remote nature of the area. Figure 6.3 does, however, underscore the necessity for knowing the nature of

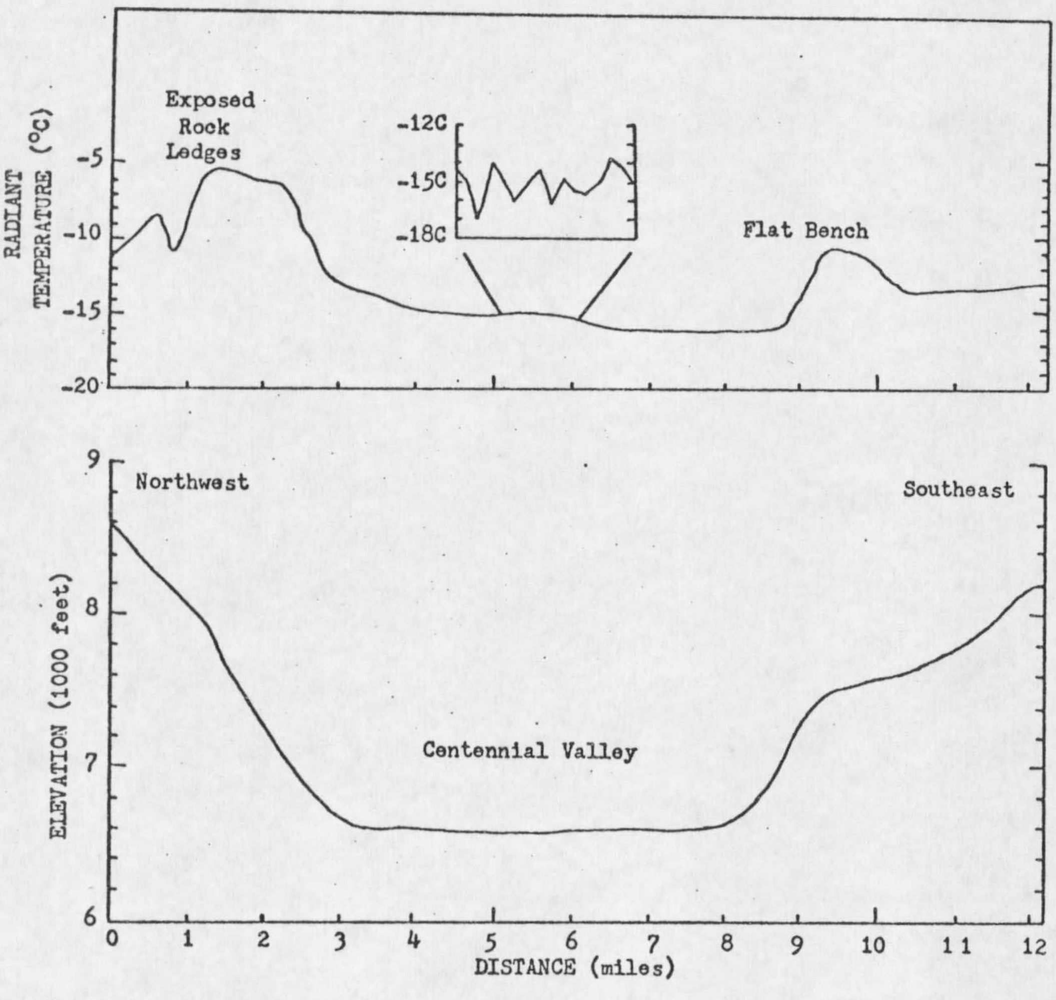

Figure 6.3 Plot of radiant snow surface temperature obtained with an airborne IT-3 radiometer in the Centennial Valley of southwestern Montana at 1220 MST on March 6, 1971. The relatively high temperatures on the northwest side of the valley are due to bare rock ledges heated by solar radiation. Inset explained in text.

the surface scanned by the radiometer. The high temperature of the rock ledges represents a significant error source if the type of surface viewed were not considered.

Three additional aerial observations of snow surface temperature were carried out, including a nighttime flight. A flight early in the afternoon of March 2, 1971, resulted in two radiometrically obtained snow surface temperatures which could be compared with air temperatures measured in weather shelters nearby. The first radiant surface temperature measurement made over a snow-covered field in the Gallatin Valley yielded a temperature of -3.3C. A thermograph housed in a weather shelter 100 yards from the flight path, approximately 1.5 meters off the surface, yielded an air temperature of -2.0C. Later the same afternoon, observations made about 1000 feet above a snow-covered mountain meadow resulted in an indicated radiant temperature of -7.0C. A thermograph at the Bangtail Mountain Observatory (BMO) located 1.5 miles from the meadow, and at a 700 foot higher elevation, recorded -7.8C for the same time period. This thermograph was housed in a weather shelter located only a few inches above the snow surface. A close correspondence between shelter temperature and radiant snow surface temperature is exhibited by the above examples.

The third series of aerial observations was made on the night of March 19, 1971, over a mountain snowfield. Conditions at the 8,000 foot BMO, located on the edge of the snowfield, included clear skies and a 20 mph wind measured 54 feet above the hard crusted snow. However, an observer on the snowfield at the time of the flight noted that the wind was nearly calm at the surface. The observer obtained a point measurement of snow surface temperature during each airborne radiometric measurement. This was accomplished by reading a precision mercury-in-glass thermometer lying on the snow surface. Although it was realized that such a measurement did not precisely determine the actual snow surface temperature, it was deemed adequate for the purposes of the aerial observation being conducted. Table 6.1 is a comparison of the temperatures obtained with the precision thermometer, the IRT, a thermograph approximately six inches off the snow surface located a quarter mile from the observer, and a thermistor in a vortex tube attached to the aircraft. Differences between "surface" temperature measured by the precision thermometer and the radiometric surface temperature varied from 0.2C to 1.9C. The IRT readings were consistently higher. A strong inversion in the first six inches above the surface is apparent from the data. The inversion extends to at least 100 feet above the snow surface. The occurrence of temperature gradients of this magnitude are a frequent phenomenon over snowfields during clear nights due to strong radiative cooling at the surface. Geiger (1966) reports a case of a gradient of up to 6C in the first millimeter above the snow surface in circumstances similar to those occurring during this night observation. Thus, considerable caution

Table 6.1 Comparison of radiant snow surface temperature, "surface" temperature obtained with a precision thermometer, shelter temperature, and air temperature at flight level over a snowfield at night.

Time (MST)	Altitude above surface (feet)	Air temperature at flight level (^oC)	Radiant snow surface temperature (^oC)	Precision thermometer "surface" temperature (^oC)	Thermograph temperature (^oC)
1915	100	-0.4	-7.1	*	-4.0
1917	300	-0.6	-7.5	*	-4.0
1920	500	-0.8	-7.8	-8.0	-4.0
1923	700	-2.0	-7.8	-8.5	-4.0
1925	900	-2.1	-8.1	-9.0	-4.0
1927	1100	-2.5	-7.8	-9.6	-4.0
1929	50	-1.3	-7.9	-9.8	-4.0

* Not available

should be exercised in extrapolating shelter level temperatures from radiometric surface temperature determinations.

During the course of the aerial measurements of snow surface temperatures, tests were conducted to ascertain the effect of atmospheric absorption and re-emission on radiometrically obtained snow surface temperatures. On two occasions aerial infrared measurements of snow surface temperature were made at altitudes varying from 100 feet to 1100 feet. Altitude changes were made in increments of 200 feet. The first test was made in the Centennial Valley at 1235 MST on March 6, 1971. The valley was under the influence of an arctic air mass and skies were clear. No change in the snow surface radiant temperature was discernable with increasing altitude to a height of 1100 feet. At that altitude observation was terminated. The second test was the observation flight on the night of March 19, 1971, near the BMO, which was discussed previously. Data from the flight are given in Table 6.1. There is no indication that the small fluctuations in radiant snow surface temperature observed with increasing altitude are associated with atmospheric absorption. Instead, the fluctuations observed are probably due to real surface temperature fluctuations and uncertainty inherent in the instrumentation. From the above results it can be concluded that atmospheric absorption for viewing distances under 1000 feet are not detectable with the system used in this study. This is not to say, however, that absorption effects are not present.

Rather, because of the limited sensitivity of the radiometer-recorder system, absorption effects under 1100 feet cannot be detected.

Airborne temperature sensing of snow-covered terrain has been shown to be a useable tool for locating surface temperature gradients and for estimating air temperature at shelter height under certain conditions. Undetected changes in the nature of the surface being viewed, e.g. snow versus trees, may lead to incongruous surface temperature patterns. It is, therefore, advisable to note terrain features as they are scanned. An even better but more expensive method would be to obtain a time synchronous photographic-temperature record by the technique described by Grossman and Marlatt (1966).

Chapter 7

SUMMARY AND RECOMMENDATIONS FOR FURTHER STUDY

The primary goal of the investigation was to determine the feasibility of remotely monitoring snow surface temperatures using an airborne infrared radiometer. The basic problem in this feasibility study was determination of the emissivity range of dry snow in the 8 to 14 micron spectral bandwidth. All radiometric measurements were made with a Barnes IT-3 Model-A infrared radiometer.

Emissivity measurements were made for 185 snow samples of varying crystalline form in the temperature range -1 to -18C. The technique utilized to perform the measurements was that of Buettner and Kern (1965), with some modification as recommended by Dana (1969). An instrument called an emissivity box was used in this approach. The vertical emissivity of snow in the 8 to 14 micron interval was found to range from 0.966 to 0.989. Freshly fallen snow exhibited an average emissivity of 0.975. Crusted snow was found to possess a mean emissivity of 0.985. The slightly higher emissivity of crusted snow may be related to the greater number of crystals per unit area and increased density. The average emissivity for all types of snow surfaces examined was 0.978. Thus, it is concluded that snow possesses approximately blackbody characteristics in the 8 to 14 micron region. Lower emissivities found in the literature appear to be incorrect.

Airborne snow surface temperature measurements were shown to be feasible and accurate to within two degrees Celsius when obtained within 1000 feet of the surface. This value includes the effect of reflected radiation from the sky, emissivity corrections, and atmospheric absorption between the target and sensor. Tops of inversions in snow-covered mountain valleys were successfully mapped during airborne case studies. This demonstrates the practical applications of radiometers for detecting air mass boundaries at their intersection with the surface. Airborne radiometric measurements of snow surface temperature were generally found to agree within 2.5C with air temperature measured in weather shelters nearby. The only exception was an instance where a strong inversion caused by radiation cooling resulted in a maximum difference of 5.8C between the radiant snow surface temperature and shelter temperature.

Radiometric temperature sensing of snow surfaces offers a useful tool in investigations of surface temperature gradients in arctic and alpine environments. Coupling an airborne infrared thermometer with an aircraft-mounted air temperature sensor provides the added capability for monitoring the temperature distribution of a remote area in three dimensions.

Airborne radiometric temperature sensing of snow-covered terrain offers a method of obtaining real-time surface temperature data in remote arctic and mountainous regions to supplement and improve satellite surface temperature information. Ultimately, satellite surface temperature monitoring on a routine basis would be preferred because of its simplicity. However, satellite scanning has the disadvantage of being limited to cloudless conditions. Airborne radiometry, on the other hand, is restricted only by flying conditions. Airborne radiometers also provide more detail on surface temperature distributions than is possible with satellite mounted sensors.

A number of possibilities for further investigation have become apparent as a result of this study. These include the following:

1. Surface temperature data acquired from satellites over snow-covered terrain should be compared with simultaneous airborne radiometric surface temperature measurements made across airmass boundaries. It may be possible to operationally detect the presence of air mass boundaries on snow-covered terrain through the use of satellite mounted sensors during clear or partially cloudy conditions. Such information could be very useful in weather forecasting, especially for regions where surface observations are sparse.

2. Airborne investigation of the three dimensional temperature structure in snow-covered mountainous regions could be undertaken. Such studies in otherwise inaccessible regions should provide insights into the complex wintertime interactions between mesoscale mountain valley weather and larger scale systems.

3. The effect of reflected radiation on infrared temperature sensing should be investigated thoroughly. This would require spectral observations of sky radiant emittance for various meteorological conditions, and evaluation of the reflected component for the filter characteristics of the radiometer employed.

4. Additional emissivity measurements should be made for other forms of ice and snow not tested in this study. The relationship between snow density, ice crystal numbers, and emissivity should be examined further. Also, emissivity measurements should be undertaken for spectral intervals other than 8 to 14 microns. With improved sensors and electronics it may be possible to restrict observations to a small band where atmospheric absorption is minimal. The atmospheric infrared window between three and four microns is such a region.

In general it can be said that remote infrared sensing over snow-covered terrain offers a convenient, mobile, and accurate means of detecting surface temperatures. This is due to the high average emissivity of snow in the 8 to 14 micron bandwidth, and the fact that the emissivity of snow remains relatively constant for differing snow crystal types. Thus, infrared radiometers, particularly in the airborne mode, are versatile and fieldworthy instruments, capable of being used for snow surface temperature measurements. Future scientific investigations should, to an increasing extent, rely on them for rapid temperature data acquisition in the field.

LITERATURE CITED

Bell, E.E., L. Eisner, J. Young, and R.A. Oetjen, 1960: "Spectral Radiance of Sky and Terrain at Wavelengths between 1 and 20 Microns. II. Sky Measurements," J. Opt. Soc. Am., V. 50, No. 12, 1313-1320.

Buettner, K.J.K., and C.D. Kern, 1965: "The Determination of Infrared Emissivities of Terrestrial Surfaces," J. Geophys. Res., V. 70, No. 6, 1329-1337.

Combs, A.C., H.K. Weickmann, C. Mader, and A. Tebo, 1965: "Application of Infrared Radiometers to Meteorology," J. Appl. Met., V. 4, 253-262.

Conway, J. and C.H.M. van Bavel, 1967: "Radiometric Surface Temperature Measurements and Fluctuations in Sky Radiant Emittance in the 600 to 1300 cm^{-1} Waveband," Agronomy Journal, V. 59, 389-390.

Dana, R.W., 1969: "Measurements of 8-14 Micron Emissivity of Igneous Rocks and Mineral Surfaces," Masters Thesis, Dept. of Atmos. Physics, Univ. of Wash., Seattle.

Dunkle, R.V., J.T. Gier, and J.T. Bevans, 1955: Final Progress Report: Snow Characteristics Project, Contract No. DA-11-190-ENG-3, 8-66-02-001, University of Calif., Institute of Engineering Research, Berkeley, Calif.

Falckenberg, V.G., 1928: "Absorptionskonstanten Einiger Meteorologisch Wichtiger Korper fur infrarote Wellen," Meteorol. Z., V. 45, 334-337.

Fleagle, R.G., and J.A. Businger, 1963: An Introduction to Atmospheric Physics, Academic Press, New York, 346 pp.

Fujita, T., G. Baralt, and K. Tsuchiya, 1968: "Aerial Measurement of Radiation Temperatures Over Mt. Fuji and Tokyo Areas and Their Application to the Determination of Ground and Water Surface Temperatures," J. Appl. Met., V. 7, 801-816.

Gates, D.M., 1961: "Winter Thermal Radiation Studies in Yellowstone Park," Science, V. 134, 32-35.

Gates, D.M., 1962: Energy Exchange in the Biosphere, Harper Row, New York, 151 pp.

Geiger, R., 1966: The Climate Near the Ground, Harvard Univ. Press, Cambridge, Mass., 611 pp.

Griggs, M., 1968: "Emissivities of Natural Surfaces in the 8- to 14-Micron Spectral Region," J. Geophys. Res., V. 73, 7545-7551.

Grossman, R.L., and W.E. Marlatt, 1966: "A Method of Showing What a Radiometer "Sees" During an Aircraft Survey," Proc. of the 4th Sympos. on Remote Sensing of the Environment, University of Michigan, Ann Arbor, 571-574.

Gubareff, G.G., J.E. Janssen, and R.H. Torborg, 1960: Thermal Radiation Properties Survey - A Review of the Literature, Honeywell Research Center, Minneapolis, Minn., 293 pp.

Holmes, R.M., 1969: "Note on Low-Level Airborne Observations of Temperature Near a Prairie Oasis," Mon. Wea. Rev., V. 97, 333-339.

Idso, S.B., and R.D. Jackson, 1968: "Significance of Fluctuations in Sky Radiant Emittance for Infrared Thermometry," Agronomy Journal, V. 60, 388-392.

Kern, C.D., 1963: "Desert Soil Temperatures and Infrared Radiation Received by Tiros III," J. Atmos. Sci., V. 20, 175.

Kern, C.D., 1965: "Evaluation of Infrared Emission of Clouds and Ground as Measured by Weather Satellites," Environmental Research Paper, No. 155, Air Force Cambridge Research Laboratories, L.G. Hanscom Field, Bedford, Mass.

Landsberg, H.E., and J.V. Mieghem, 1970: Advances in Geophysics, V. 14, (Precision Radiometry, ed. A.J. Drummond), Academic Press, New York, 415 pp.

Lenschow, D.H., and J.A. Dutton, 1964: "Surface Temperature Variations Measured from an Airplane Over Several Surface Types," J. Appl. Met., V. 3, 65-69.

Lorenz, D., 1966: "The Effect of the Long-wave Reflectivity of Natural Surfaces on Surface Temperature Measurements Using Radiometers," J. Appl. Met., V. 5, 421-430.

Magono, C., and C.W. Lee, 1968: Meteorological Classification of Natural Snow Crystals, U.S. Dept. of Agri., Forest Service, Alta Avalanche Study Center, Wasatch National Forest.

Reprinted from J. of the Faculty of Science, Hokkaido Univ., Series VII (Geophysics), V. 2, No. 4, Nov., 1966.

McAlister, E.D., 1964: "Infrared-Optical Techniques Applied to Oceanography, 1, Measurement of Total Heat Flow from the Sea Surface," Appl. Optics, V. 3, 609-612.

Miller, C.D., 1963: "An Airborne Spectral Radiometer," Proc. of 2nd Sympos. on Remote Sensing of Environment, Univ. of Mich., Ann Arbor, 359-372.

Schaefer, V.J., 1949: "The Formation of Ice Crystals in the Laboratory and the Atmosphere," Chemical Rev., V. 44, 291-320.

Snow Hydrology, North Pacific Division, U.S. Army Corps of Engineers, 1956: Portland, Oregon.

Valovcin, F.R., 1968: "Infrared Measurements of Jet Stream Cirrus," J. Appl. Met., V. 7, 817-826.

Wark, D.Q., G. Yamamoto, and J.H. Lienesch, 1962: "Methods of Estimating Infrared Flux and Surface Temperatures from Meteorological Satellites," J. Atmos. Sci., V. 19, 369-384.

Weingeroff, 1931: "Uber dat Reflectionsvermogen von Wasser und Eis im Ultrarot," Z. Physik, V. 70, 104-108.

Wolfe, W.L., 1965: Handbook of Military Infrared Technology, Office of Naval Research, Washington, D.C., 906 pp.